

## **Submission to Queensland Floods Commission of Enquiry**

### **Terms of Reference: Section 2. e) adequacy of forecasts and early warning systems**

This submission is made with the purpose to identify that knowledge existed in 2009 that precisely determined that beginning in circa 2010, significant high rainfall and severe weather events would occur, but authorities refused to reply or acknowledge such data.

Although such knowledge could not have prevented the high rainfall and subsequent floods of 2011, and Cyclone Yasi, there existed a very high level of probability determined by pure scientific data, and not personal opinion, weather forecasting, or computer modelling, that such events would have to occur, commencing circa 2010, and continuing until circa 2015. If the population or authorities had been made aware of such probability, and order of magnitude, from late 2009 when it was available, it is reasonable to consider that such loss of personal assets and life could have been avoided. It is within this context that this submission is made.

The information pertaining to the above was discovered in 2006. An abstract of the scientific paper detailing the data, titled *Global Warming Trigger Event* has been accepted, and the final paper submitted, for presentation to the forthcoming 34<sup>th</sup> World Congress of the International Association for Hydro-Environment Engineering and Research, 26<sup>th</sup> June, at the Brisbane Convention and Exhibition Centre.

A paper titled *The Cause and Effect of Global Weather Change V1.0*, has been submitted to the World Academy of Science for acceptance for the 2011 International Conference on Climate Change and Global Warming conference in Venice.

### **Background**

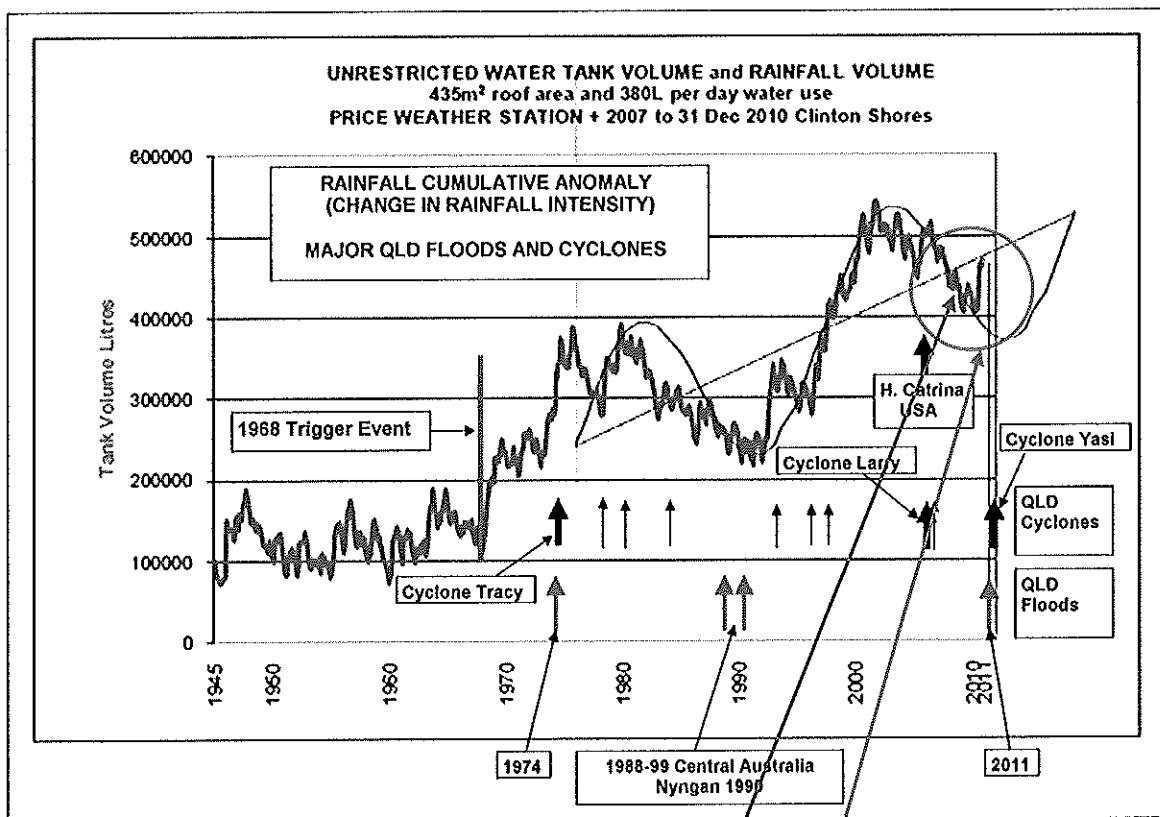
In 2005 the design began for the first rainwater self-sustainable residential subdivision to be approved by the Development Assessment Commission and SA Water in South Australia ([www.clintonshores.com.au](http://www.clintonshores.com.au)). As part of that design it was necessary to investigate historical rainfall patterns, and explain how 'Global Warming' was having an impact on rainfall. An outcome of that investigation was the discovery of significant data embedded within the historical rainfall data that showed the origin of Global Warming. In particular it showed that there had commenced a global weather oscillation that had caused the previous severe 'drought', and would from circa 2010, cause severe increase in rainfall and weather events.

The design engineer who discovered the data, Darryl Whitford, has been a research and development engineer for over 40 years. He has been awarded the highest environmental award in Australia, the Banksia Environmental Award for his prior work in water management; and numerous other industry awards, including the Australian Newspaper Computer Software Awards six times between 1991 and 1995. Darryl has no political position, or particular interest in Global Warming.

## The Data

It must be noted that the data discovered is not 'forecast' data, but rather concise weather change operating to defined Simple Harmonic Motion. Since 2006, the rainfall at Price Weather Station (South Australia) accurately followed such change, confirming the discovery, and accurately determining that from circa 2010 such extreme weather events as described had to occur.

The following is an extract from the paper *The Cause and Effect of Global Weather Change V3*, Page 18. It shows the discovered weather oscillation, and relation of significant Queensland floods and Cyclones from 1974 to date. Cyclone Tracy and Hurricane Katrina are also shown.



It is not the intention to discuss the data in this document, however the paper *The Cause and Effect of Global Weather Change V3* which is appended to this submission, explains that during the transition of the weather oscillation during the period (here) that rainfall has to increase substantially in order for the rainfall oscillation (here) to change direction from a negative to a positive transition. From 2010 this change becomes substantial. During the negative transition, there exists positive feedback in 'Global Warming', causing extreme weather events. This period of 2005 to 2010 is reflected in the period 1985 to 1990, when less severe floods occurred. The paper *The Cause and Effect of Global Weather Change V3* gives the reasons why the magnitude of the rainfall and weather events (globally) have increased during the second oscillation cycle.

In 2009, with the realisation of the weather sine oscillation that had commenced in 1985, it was able to accurately determine what the weather variation would have to be in order to follow the sine curve. In practice since 2006 the rainfall has accurately followed the sine curve, determining the accuracy for the extreme rainfall events that had to commence from 2010.

### **Resistance to Knowledge**

It was the intention to publically disseminate this knowledge for peer review and public discussion from late 2009, however substantial opposition to accept any data that did not comply to the 'accepted' concept of Global Warming based on Carbon Dioxide cause was encountered by the CSIRO and others, including the media. A web site [www.globalwarmingtriggerevent.com](http://www.globalwarmingtriggerevent.com) was established in October 2009, with download copies of the technical papers available.

The CSIRO refused to reply to requests for discussion on the data. The earliest submission to the CSIRO was made in July 2008 to the CSIRO Centre for Australian Weather and Climate Research without any reply, and to Dr Andrew Johnson, Group Executive of the CSIRO Environment Group on 1/2/2010, without reply.

A submission of the paper *The Cause and Effect of Global Weather Change V1.0* to the Australian Government and CSIRO GREENHOUSE2011 conference in Brisbane, 2011, was rejected on the 15/12/2010.

Attempts to disseminate the information to most political groups proved fruitless. Despite several attempts to inform the Opposition (Liberal Party) of the information; that included direct email to the Liberal party, Tony Abbot, and a personal delivered printed copy to the local member for Grey, no response could be obtained.

The main-stream media, and personalities who dominate Global Warming and current affairs discussion have been sent the information, with mostly no reply, and no publication.

The foregoing discussion is given as examples of how real data that may contribute to understanding and the ability to determine when severe weather events may or will occur is deliberately excluded from discussion and dissemination.

*If the data is correct, the floods of 2011 and severe weather events such as Cyclone Yasi in Queensland have the capability to continue to circa 2015 and intensify.*

*After the next peak of the weather oscillation is reached, a severe drought, orders of magnitude worse than that experienced over the last decade is likely to occur.*

*Indications are that the oscillation is increasing in magnitude, driven by positive Global Warming feedback. If this is true, then the magnitude of high rainfall and extreme weather events, and the intensity of the drought period will increase substantially.*

## **ATTACHMENTS**

### **ATTACHMENT A**

**Paper titled 'The Cause and Effect of Global Weather Change'.**

# The Cause and Effect of Global Weather Change

D.R. Whitford

**Abstract**—Data from the Australian Bureau of Meteorology shows that the weather variation known as ‘Global Warming’ began with a Trigger Event. Large quantities of white phosphorus that were used in Vietnam between 1965 and 1968 correlate with severe changes to the previous simple harmonic variation in the rainfall. The hygroscopic aerosols of phosphorus pentoxide contaminated the global atmosphere, causing significant increase in rainfall. The data shows that after 1968, the timing and the rate of change of global temperature correlate exactly with the rainfall variations. Increase in rainfall anomaly can be shown to cause increase in atmospheric Carbon Dioxide. Increases in Global ecosystem phosphorus contamination correlate precisely with the Trigger Event. The Trigger Event hypothesis has been used to accurately predict rainfall since 2006, and directly links a cause to Global Warming. The Trigger Event hypothesis is supported by observed data and no computer modelling is used.

**Keywords**— global warming, trigger event, rainfall oscillation, phosphorus pentoxide.

## I. INTRODUCTION

In 2005, the engineering design began for what was to become the first water self-sustainable residential development to be approved in South Australia, the Clinton Shores residential development at Port Clinton, Yorke Peninsula [1]. In order to understand water sustainability, it was necessary to understand the historical rainfall pattern for the region, and how Global Warming had altered rainfall in recent years. The roof area of a dwelling was calculated to be that which would give the required amount of household daily water-use based on receiving the daily average rainfall. The water tank volume was calculated from the equation:

$$\text{Tank Volume (L)} = (\text{starting volume of tank (100,000L)}) + (\text{monthly rainfall volume (L) input from the home roof and water tank (= roof area X per month total rainfall in mm)}) - ((\text{monthly water used every month in the home (= roof area X overall average monthly rainfall in mm)}))$$

The water obtained from the average rainfall should equal the water being used by the dwelling, so the volume of the rainwater tank should remain the same over a long time period unless there were substantial changes in rainfall.

In 2006 the monthly rainfall records for the period from 1945 to 2006 inclusive, for the Price Weather Station from the Australian Bureau of Meteorology was obtained [2]. Price is 6km from the Clinton Shores development. The rainfall data for June 2006 to Dec 2006 was obtained independently at Clinton Shores to complete the 2006 Price data set. The annual rainfall totals for Price depicted the characteristics as shown in Fig. 1.

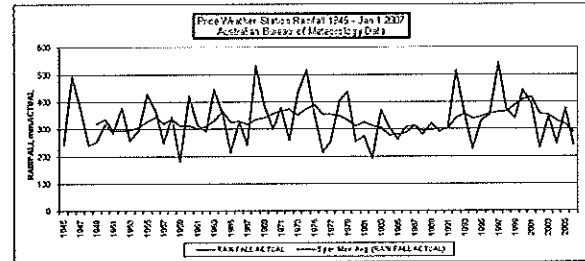


Fig. 1 Rainfall Variation 1945 to 2007 Price Weather Station and Clinton Shores.

The rainfall from 1945 to 1965 was reasonably stable about the Trend Line, but there existed some variability in the data post 1965, that showed exceptional rainfall variations over long time periods, occurred from 1965 to 2007. It had been determined that a dwelling would need a roof area of some 435m<sup>2</sup> in order to obtain adequate water from the 1945 – 1965 average rainfall period, taken as representative of ‘pre Global Warming’. The water tank volume was plotted as monthly intervals against a dwelling roof area of 435m<sup>2</sup> and 380L per day water use, the best calculation of the available water use for the 1945 – 1965 average rainfall period, for the period of 1945 to August 2010.

## II. DATA DISCOVERY

The result in Fig. 2 showed significant more detail in the rainfall characteristic. The period 1945 – 1965 returned an almost null average change in water tank volume, except for regular periods of alternating rainfall, but the exceptional rainfall periods were more enhanced. The water tank volume showed that there was an increase in the volume of water of 327,890 litres over the 64 years from 1945 to 2010.

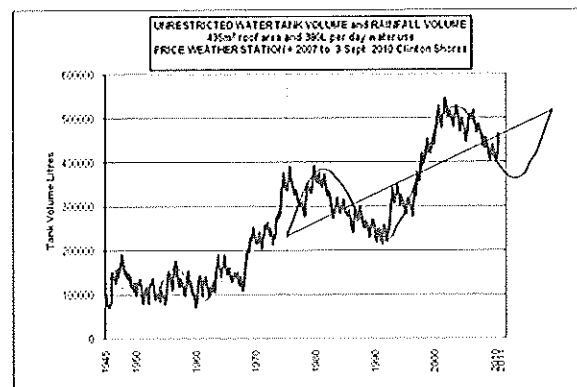


Fig. 2 Water Tank Volume.

Fig. 2 displays the total gain in rainfall from 1968 to 2010 and characteristics associated with that gain. Changes in rainfall

D.R. Whitford is with Clinton Shores Developments Pty Ltd, Port Clinton, South Australia, Australia, 5570. (e-mail: [dwhitford5@bigpond.com](mailto:dwhitford5@bigpond.com)). V3.0 4-2-2011

characteristics and increase of rainfall occurred precisely at 1968. From 1968, the rainfall showed extraordinary characteristics of periods of higher, increasing rainfall, and lower, reducing rainfall, over a time period of 24 years. This behaviour was initiated by an extraordinary Trigger Event from 1968, although closer examination can show that the rainfall was beginning to increase from 1965 onwards. From 1968 there was an overall increase in total rainfall, evidenced by the fact that from 1968, the water tank volume, reasonably constant since 1945, increased in volume because the total rainwater being input had become more than was being used.

Almost everything in nature conforms to basic fundamental mathematically defined functions. One of these functions is Simple Harmonic Motion most commonly known as a sine wave oscillation. Note that although a sine wave can have a large 'high' and 'low' value swing, the average value over a full sine wave cycle is a straight line through the centre of the oscillation. It was observed that the extraordinary rainfall variation since 1968 closely represented a sine wave. There is also evidence that there existed from 1945 a smaller sine wave event in rainfall variation.

By superimposing a sine wave curve (adjusted for positive axis slope) over the rainfall variation, it can be seen in Fig. 4 that the rainfall variations have become a true sinusoidal function, with the rainfall data perfectly following a sine function by the second cycle. Fitting the sine function to the rainfall variation also determines the positive slope of the mean rainfall variation.

The low amplitude, higher frequency, oscillation from 1945 can be seen, along with the extraordinary increase in sinusoidal variation from 1968. The low amplitude variations can be seen to continue to be superimposed upon the larger sine variation. The lower amplitude, higher frequency variation represents the historically normal periodic weather variations, while the larger amplitude, lower frequency variations represents extraordinary variations in rainfall.

### III. NORMAL PERIOD OF WEATHER

The Normal Period used for the Australian and South Australian Rainfall data is based on the 1961 to 1990 reference period [3],[4]. This period contains a significant Outlier, shown as 1973 – 1975 in Fig. 3(a). Other than being a statistical Outlier, the Outlier is actually an abnormal event as it comprises the first rainfall oscillation event in Fig. 2. This Outlier causes an abnormal negative offset to all other rainfall data using the 1961 to 1990 Normal Period Reference.

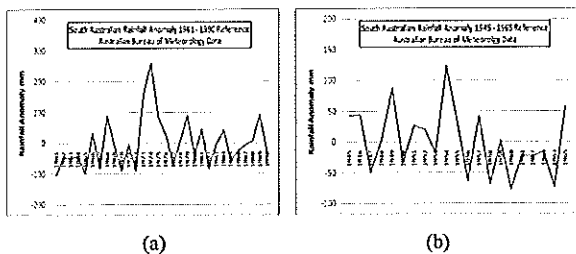


Fig. 3 South Australian 1961 -1990 and 1945-1965 Normal Period Comparison

The 1945 to 1965 Normal Period shown in Fig. 3(b) was chosen as the reference to present much of the data in this paper as it is a period considered to contain a normal distribution [5].

### IV. RAINFALL CUMULATIVE ANOMALY

Rainfall variation can be expressed as a total over time. If the average rainfall was 5mm per month, then by taking the average rainfall away from each month rainfall total the rainfall variation, or anomaly from the average value of rainfall, is derived.

If there were over a period of time, equal average increase and equal average decrease in rainfall, then the cumulative anomaly would be a horizontal line, showing short term variations in rainfall, but there would be no sustained increase or decrease in the results. The water tank volume of Fig. 2 is effectively the cumulative anomaly of rainfall because the daily water use is equal to the average daily rainfall for the 1945 to 1965 period.

Fig. 4 shows the rainfall anomaly for Price weather station using the 1945 to 1965 Normal Climate reference period. It closely conforms to the water tank volume data of Fig. 2.

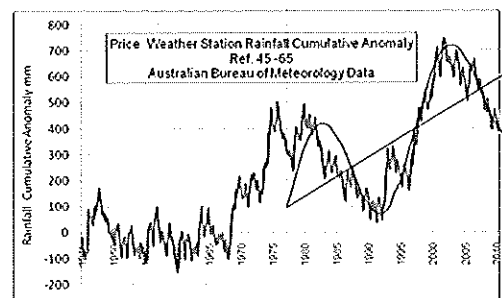
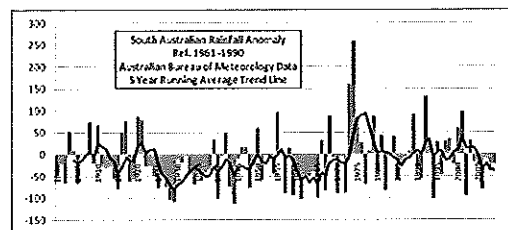


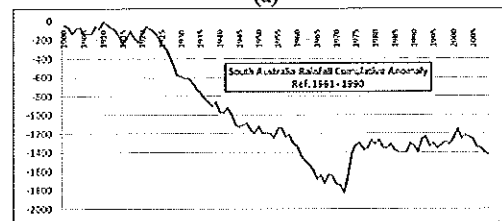
Fig. 4 Price Rainfall Anomaly. Ref: 1945 – 1965.

### A. South Australian Rainfall Anomaly

The Australian Bureau of Meteorology South Australian yearly rainfall anomaly supports the Price rainfall data [8]. The high rainfall event of post 1968 is clearly seen in Fig. 5(a) [4].



(a)



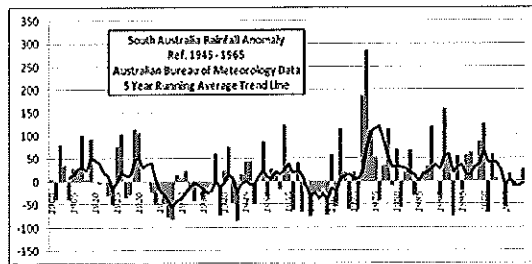
(b)

Fig. 5 South Australia Rainfall Anomaly. Ref: 1961 – 1990

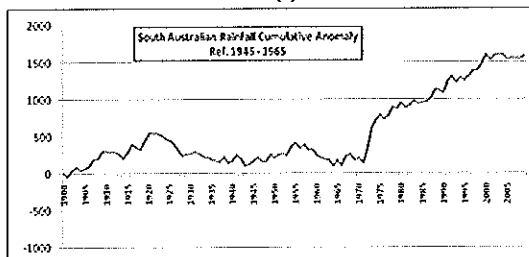
The South Australian rainfall anomaly represents variation in rainfall to a reference period of 1961 to 1990. It can be seen that substantial rainfall increase events occurred after 1968. If the anomaly value for each year of the rainfall anomaly graph is

progressively added to generate a Cumulative Anomaly, the result in Fig. 5 is obtained.

In practice it would be highly unlikely for a total of -1400mm of negative rainfall anomaly between 1920 and 1970 as shown in Fig. 5. to occur. This aberration is due to the Normal Period reference chosen of 1961 to 1990 causing the period of 1924 to 1972 to be below the base reference line, generating negative anomaly numbers. The 1961 to 1990 period contains a significant outlier of high rainfall, causing the average value of the 1961 to 1990 period to be higher. If the Normal Period reference of 1945 to 1965 is used to readjust the South Australian rainfall anomaly, the results are as per Fig. 6(a). The South Australian Cumulative Rainfall Anomaly of



(a)



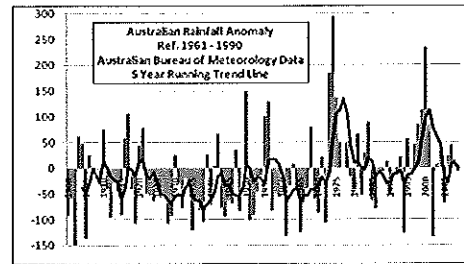
(b)

Fig. 6 South Australian Rainfall Anomaly. Ref: 1945 – 1965

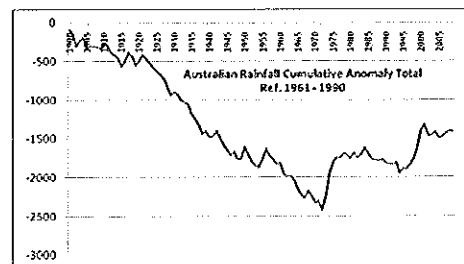
Fig. 6(b) shows that at circa 1970 the Cumulative Rainfall Anomaly maintains a positive anomaly in rainfall. Note at precisely 1916 an increase in positive rainfall anomaly also occurs.

### B. Australian Rainfall Anomaly

The Australian Bureau of Meteorology Australian yearly rainfall anomaly as shown in Fig. 7(a) supports the Price rainfall data [3]. The high rainfall event of post 1968 is clearly seen in Fig. 7(a). The rainfall peaks of circa 1976 and 2000 corresponding to the sine wave peaks of Fig. 4 are clearly evident. Adjusted for the Normal Period reference of 1945 to 1965 the Australian Rainfall Anomaly is as per Fig. 8(a). The Australian Cumulative Anomaly of Fig. 8(b) shows that at circa 1970 the cumulative anomaly maintains a positive anomaly in rainfall to 2010. Note at precisely 1916 an increase in positive rainfall anomaly also occurs.

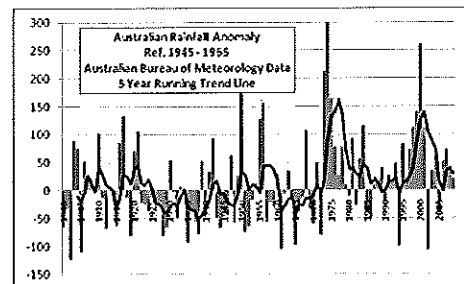


(a)

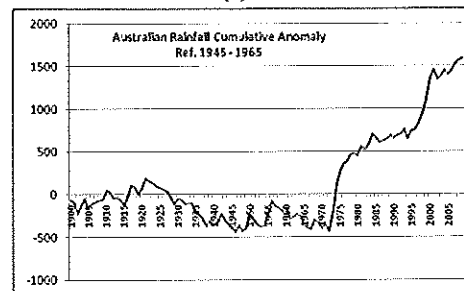


(b)

Fig. 7 Australian Rainfall and Cumulative Anomaly. Ref: 1961 – 1990



(a)



(b)

Fig. 8 Australian Rainfall and Cumulative Anomaly. Ref: 1945 – 1965

## V. AUSTRALIAN TEMPERATURE ANOMALY CORRELATION TO RAINFALL ANOMALY

Fig. 9 shows the correlation of the Price Cumulative Rainfall Anomaly (as empirical water tank volume) against the Australian Temperature Anomaly [6]. Simple Harmonic sine wave functions have been superimposed over the data where appropriate.

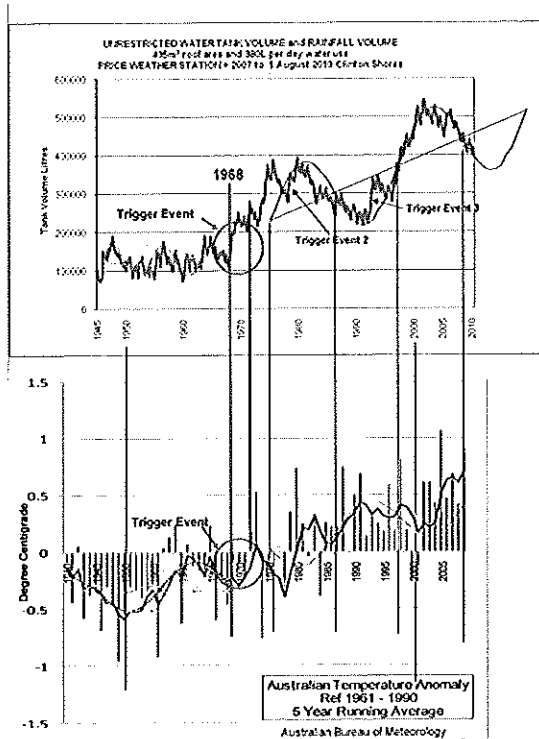


Fig. 9 Correlation of Price Rainfall Anomaly to Australian Temperature Increase

Fig. 9 shows that there is a direct correlation to the rainfall anomaly increase that has occurred after 1968 and the increase in Australian temperature anomaly. The sine wave oscillation of the rainfall Cumulative Anomaly for Price occurs at precisely the same timeline as the Australian temperature anomaly increase for 1945 to 2010.

From 1945 to 1968, both the Price rainfall Cumulative Anomaly and the Australian temperature anomaly exhibited a flat mean variation. From 1945 to 1968, both the Price rainfall Cumulative Anomaly and the Australian temperature anomaly exhibited stable sine wave oscillation.

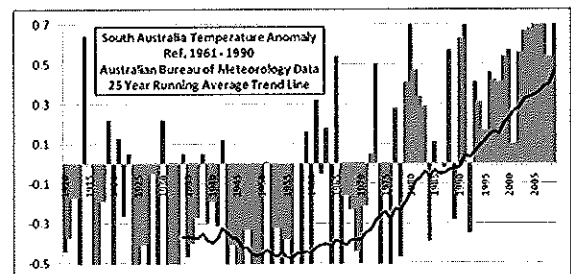
From 1965 to 1968 both the Price rainfall Cumulative Anomaly and the Australian temperature anomaly exhibit a mean linear increase in value. At 1968 a Trigger Event initialised a significant increase in Price rainfall Cumulative Anomaly, associated with a direct increase in the Australian temperature anomaly. The Trigger Event initialised the commencement of a significant oscillation in rainfall at Price.

By 1985, the oscillation had stabilised to form a pure sine wave Simple Harmonic Function. From 1985 to 2010 the rainfall

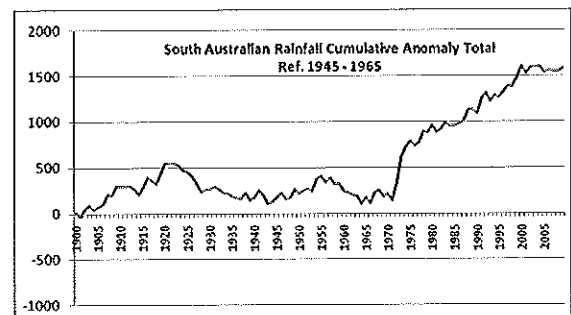
Cumulative Anomaly at Price has accurately followed the sine wave function. Fig.9 shows an inverted sine wave function placed on the Australian temperature anomaly in the same timeframe as the Price rainfall Cumulative Anomaly.

The temperature increase of the Australian temperature anomaly from 1968 to 2010 constitutes all of the temperature increase attributed to global warming from 1945. The Trigger Event at 1968 caused a significant disruption to the World's Simple Harmonic oscillation of temperature. The frequency of the initiated Trigger Event rainfall Simple Harmonic oscillation at 1968 at Price is the same as the Australian temperature anomaly Simple Harmonic oscillation. This oscillation did not exist prior to 1968.

It is evident In Fig. 10 from the comparison of the South Australian Temperature Anomaly and the South Australian Cumulative Rainfall Anomaly, that a change in both rainfall and temperature anomalies occurs at a precise period of time, at circa 1968, or immediately thereafter [7]. There was no significant increase of temperature prior to precisely 1968. Note there was an increase in the South Australian Cumulative Rainfall Anomaly Fig. 10(b) at circa 1916.



(a)

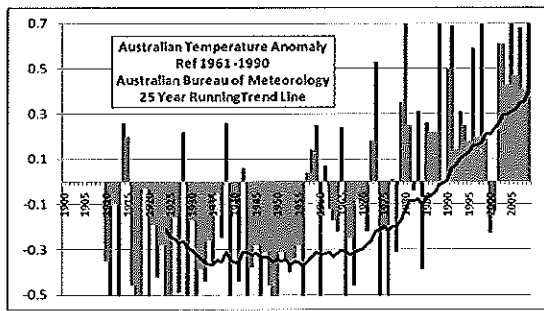


(b)

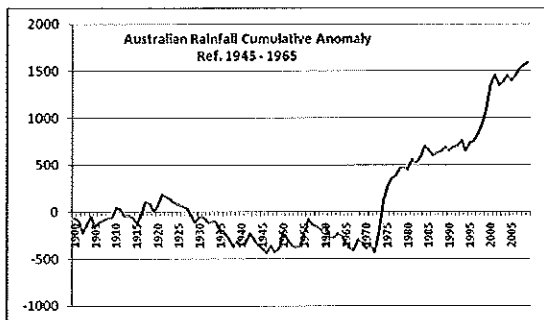
Fig. 10 South Australia Temperature Anomaly and Rainfall Cumulative Anomaly.

It is evident In Fig. 11 from the comparison of the Australian Temperature Anomaly and the Australian Cumulative Rainfall Anomaly, that a change in both rainfall and temperature anomalies occurs at a precise period of time, at circa 1968, or immediately thereafter. There was no significant increase of temperature prior to precisely 1968. Note there was an increase in the Australian Cumulative Rainfall Anomaly Fig. 11(b) at circa 1916.





(a)



(b)

Fig. 11 Australian Temperature Anomaly and Rainfall Cumulative Anomaly.

## VI. LATENT HEAT OF PRECIPITATION

It is the Latent Heat of rainfall that drives the powerhouse of the World, providing the thermal energy that creates the World's atmospheric circulation and weather.

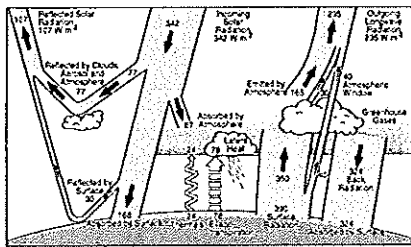


Fig. 12 The Mean Annual Radiation and Heat Balance of the Earth (Kiehl, J.T. and Trenberth, K.E., 1997)

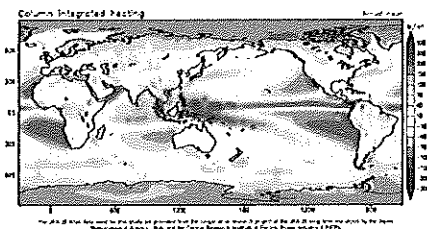


Fig. 13 Column Integrated Heating (JRA-25 Atlas (2010))

Shown in Fig. 12, the Latent Heat of rainfall is one of the main causes of heating in the atmosphere, releasing large amounts of energy as heat [8]. The majority of the heating as shown in Fig. 13 is

due to Latent Heat from rainfall, as high as  $500\text{W/m}^2$  in the tropical regions [9].

The continuous and sustained increase in precipitation from the Trigger Event to 2010 has resulted in an increase of Latent Heat release after 1968, due to increased rainfall events. While latent heat release in the atmosphere is accompanied by equivalent latent heat absorption due to water evaporation from the oceans, higher latent heat release due to higher rainfall has to cause a greater differential in temperature between the atmosphere where precipitation occurs, and the primarily water surface of the oceans where water evaporates.

The higher Latent Heat release will also create higher atmospheric turbulence leading to more severe storms, as it is the Latent Heat release from rainfall that creates much of the energy of the World's wind and weather systems.

The increase in rainfall from 1968 to 2010 has resulted in an overall increase in temperature differential between the atmosphere and the earth's surface. At Clinton Shores a hypothetical dwelling water collection site as per Fig. 2 had an increased accumulation of 300,000L of water from 1965 to 2010. This equates to a thermal energy release of Latent Heat of  $678 \times 10^6 \text{ kJ}$ , or  $1.5586 \times 10^6 \text{ kJ/m}^2$  of the earth surface. This differential has to result in a warmer atmosphere which in turn can increase the amount of water vapour and increased atmospheric heating due to the Greenhouse Effect, leading to a positive feedback effect.

## VII. WATER VAPOR

Water vapor content of the atmosphere has the greatest effect on the Greenhouse Effect.

Water vapor accounts for the largest percentage of the greenhouse effect, between 36% and 66% for clear sky conditions and between 66% and 85% when including clouds. Water vapor concentrations fluctuate regionally, but human activity does not significantly affect water vapor concentrations except at local scales, such as near irrigated fields. According to the Environmental Health Center of the National Safety Council, water vapor constitutes as much as 2% of the atmosphere.

The Clausius-Clapeyron relation establishes that air can hold more water vapor per unit volume when it warms. This and other basic principles indicate that warming associated with increased concentrations of the other greenhouse gases also will increase the concentration of water vapor. Because water vapor is a greenhouse gas this results in further warming, a "positive feedback" that amplifies the original warming. This positive feedback does not result in runaway global warming because it is offset by other processes that induce negative feedbacks, which stabilizes average global temperature [10].

For an oscillation to occur and to be maintained there has to be positive feedback of energy. If the Trigger Event oscillation was to cause periods of higher water vapor in the Atmosphere as part of its sine wave transition, obtaining more energy as part of the Greenhouse Effect would constitute positive feedback.

During the positive swing of the sine wave oscillation of Fig. 2 (from lowest trough to highest crest), as the rainfall increases, so too will the temperature of the upper atmosphere, causing more water vapor to be held. During the negative swing of the oscillation, (assuming that the positive swing, as it nears the apex, will have consumed water vapor), water vapor may be building up as the negative swing progresses towards the bottom trough of the negative swing.

There is evidence that the water vapor increase associated with Greenhouse energy increase occurs during the negative sine oscillation. In Fig. 2 there is indication that the oscillation initiated at the Trigger Event in 1968, first entered into a pure sine

oscillation at the lower section of the negative oscillation, shortly after the zero crossing from the positive cycle.

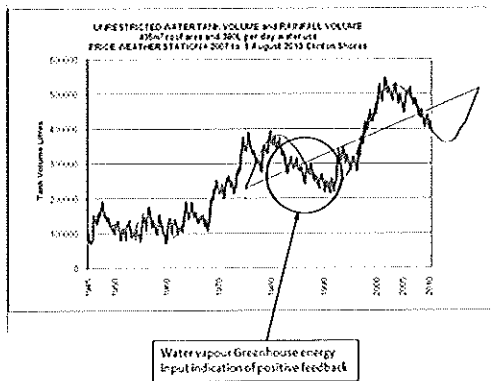


Fig. 14 Indication of Positive Water Vapour Greenhouse Energy Feedback

VIII. TRIGGER EVENT CAUSE

There are three unique discernable trigger events that occur between 1968 and 2010, referred to in Fig. 15 as the Trigger Event, Trigger Event 2, and Trigger Event 3.

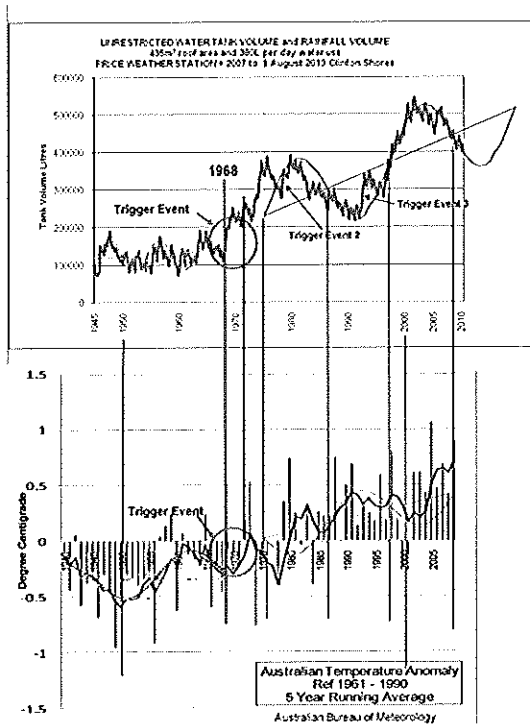


Fig. 15 Trigger Event

There is one event that correlates precisely with the primary 1968 Trigger Event, as implausible as it may initially seem.

In the Vietnam War, America conducted the 'Rolling Thunder' bombing offensive. Originally intended to only last a short time, it however, resulted in continuous bombing from March 1965 to October 1968. 1,000,000 tons of bombs were dropped on Vietnam during the Rolling Thunder campaign [11]. Many of the bombs were white phosphorus bombs [12]. It is extremely probable that the large

amount of phosphorus and its by-products such as phosphorus pentoxide, contaminated the world's atmosphere and increased rainfall by atmospheric seeding.

White phosphorus is a common allotrope of the chemical element phosphorus which has found extensive military application as an incendiary agent, smoke-screening agent, and as an antipersonnel flame compound capable of causing serious burns. It is used in bombs called phosphorus bombs, which burst into flames upon impact. White phosphorus has been called a chemical weapon by many people and organizations, including members of the United Nations. It is commonly referred to in military jargon as "WP". The Vietnam War era slang "Willy(i)e Pete" or "Willy(i)e Peter" is still occasionally heard.

Weight-for-weight, phosphorus is the most effective smoke-screening agent known, for two reasons:# It absorbs most of the screening mass from the surrounding atmosphere; and# The smoke particles are actually an aerosol, a mist of liquid droplets which are close to the ideal range of sizes for Mie scattering of visible light. This effect has been likened to three dimensional textured privacy glass—the smoke cloud does not obstruct an image, but thoroughly scrambles it. It also absorbs infrared radiation.

When phosphorus burns in air, it first forms phosphorus pentoxide (which exists as tetraphosphorus decoxide except at very high temperatures)::  $P_4 + 5 O_2 \rightarrow P_4O_{10}$ . However phosphorus pentoxide is extremely hygroscopic and quickly absorbs even minute traces of moisture to form liquid droplets of phosphoric acid::  $P_4O_{10} + 6 H_2O \rightarrow 4 H_3PO_4$  (also forms

polyphosphoric acids such as pyrophosphoric acid,  $H_4P_2O_7$ ) Since an atom of phosphorus has an atomic mass of 31 but a molecule of phosphoric acid has a molecular mass of 98, the cloud is already 68% by mass derived from the atmosphere (i.e. you have 3.2 kilograms of smoke for every kilogram of WP you started with); however, it may absorb more because phosphoric acid and its variants are hygroscopic. Given time, the droplets will continue to absorb more water, growing larger and more dilute until they reach equilibrium with the local water vapour pressure. In practice, the droplets quickly reach a range of sizes suitable for scattering visible light and then start to dissipate from wind or convection" (All Experts, 2009) [12].

It is highly probable that phosphorus pentoxide could have caused atmospheric rain seeding to occur. In Tasmania in Australia, aircraft are used to seed Silver Iodide into the atmosphere to increase rainfall for the hydro electric catchment. Tasmania uses 150 grams of Silver Iodide for three and three quarters of an hour aerial seeding, with a total of 107 hours per year, using 4.28kg of Silver Iodide to seed 2,500 sq kilometres and create 5% increase in rainfall [13].

If only 100,000 tons (US) of the 1,000,000 tons of bombs in the Rolling Thunder campaign were White Phosphorus, 100,000 tons (US) is 90,718,400 kg. It is probable that the tonnage is much higher than this.

The white clouds from the White Phosphorus bombs as shown in Fig. 16 are an aerosol mist. The white 'smoke' is instantaneous atmospheric water vapour to liquid water conversion from the hygroscopic phosphorus pentoxide produced as a result of the burning phosphorus. The pure white explosions are phosphorus bombs. Film records of Vietnam bombing show significant white phosphorus use [14]. The orange explosions are Napalm, but a phosphorus bomb is used to ignite the Napalm.



Fig. 16 Phosphorus Bomb Explosions Vietnam

If the Price Cumulative Rainfall Anomaly data is expanded as in Fig. 17, the timing relationship between the Rolling Thunder bombing in Vietnam and the increase in rainfall can be seen. The moving average line on the graph is the average of 60 data points (5 year running average). It clearly shows that the rainfall increased as a distinct event precisely being initiated at the Rolling Thunder event. Rainfall had begun to increase from 1965 before the Trigger Event. After the Trigger Event, the rainfall increased at a mean linear rate from 1968.

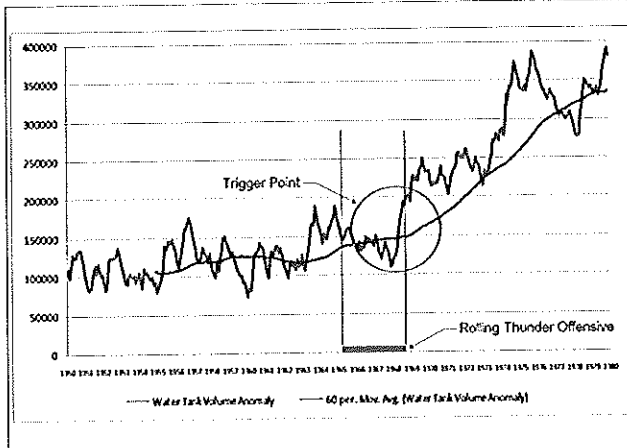


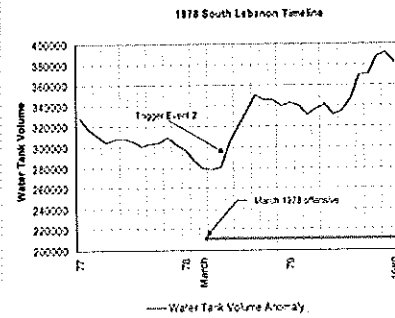
Fig. 17 Trigger Event Timeline Correlation

In Fig. 15 the circa 1978 rainfall can be seen to decrease, but then to suddenly increase again, referred to in Fig. 15 as the Trigger Event 2. Shown in Fig. 18(a), this event exactly coincides with the 1978 South Lebanon conflict, almost to the exact month. In 1992 the rainfall can again be seen to increase rapidly, referred to in Fig. 15 as the Trigger Event 3. Shown in Fig. 18(b) this event exactly coincides with the 1992 to 1995 Bosnian War. Both these trigger events have an association with reported white phosphorus bombing [12]. There are numerous Internet sites that refer to white phosphorus bombs being used in both these conflicts, particularly as they are seen as chemical weapons. These trigger events may have added to the probably already contaminated atmosphere from the Vietnam conflict, causing the rainfall and weather pattern to be re-excited in a 23 year period oscillation of significant magnitude.

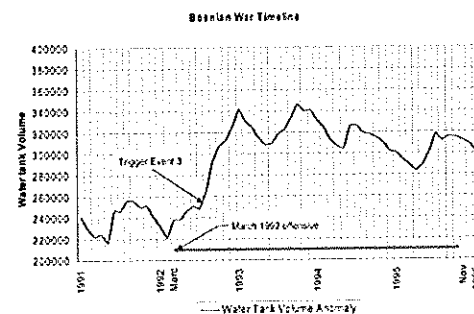
### IX. PHOSPHORUS CORRELATION TO TRIGGER EVENT

There are many scientific papers across multi disciplines that refer to high levels of phosphorus post 1968. Multiple global ecosystem studies show unexplained exceptional high phosphorus levels post 1968. The high phosphorus levels have changed the ecology, effecting many ecosystems. It is accepted that high phosphorus levels can occur due to agriculture fertiliser runoff and sewerage contamination, however many studies in often remote regions show the same phosphorus timeline of concentration increase post 1968 across the globe. Some studies determine that the increase in phosphorus is inconsistent with run off contamination, or can only provide a hypothesis as to the cause of the increase.

It can reasonably be concluded that if it can be shown that there is a consistency of correlation of high phosphorus contamination across global regions post 1968 then the phosphorus contamination of the Rolling Thunder Vietnam campaign can be shown to have contaminated the Earth Atmosphere.



(a)



(b)

Fig. 18 South Lebanon and Bosnia Timeline Correlations

The information following is from some excellent research papers. Fig. 19 shows a significant and erratic increase in phosphorus at Lake Geneva, at precisely the 1968 Trigger Event time line [15]. Atmospheric contamination of phosphorus between 1965 and 1968 in Vietnam would have resulted in an extended deposition and eventual decline in atmospheric phosphorus input to ecosystems precisely as shown in Fig. 19. Note the increase of phosphorus from circa 1965, as the Rolling Thunder campaign commenced in 1965.

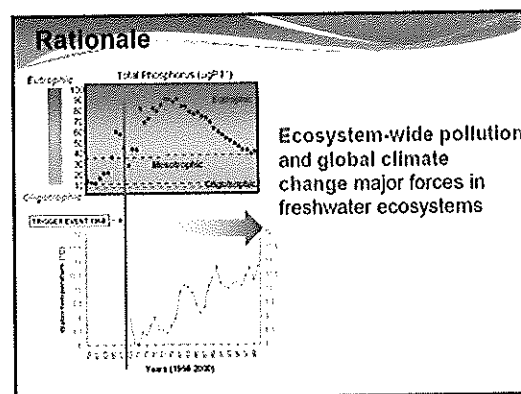
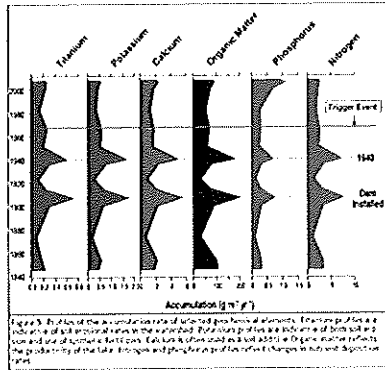


Fig. 19 Phosphorus Pulse, Lake Geneva, after 1968 Trigger Event (Molinero, C., 2009)

Fig. 20 shows an increase in phosphorus that is not consistent with soil erosion or runoff. Using titanium as an indicator, it is possible to determine the importance of soil erosion as a phosphorus source. The ratio of titanium to phosphorus declines after 1970 indicating that much of the phosphorus that entered the lake during

the last 4 decades is not from soil erosion since a decline in the ratio indicates that phosphorus levels are increasing at a rate faster than soil erosion. Although it is likely that fertilizers contribute some of the phosphorus, the decline in the ratio of potassium to phosphorus after 1950 indicates that the fertilisers are not a large source of phosphorus. It is not clear what the source of elevated phosphorus is after 1980, on possibility is internal loading of phosphorus [16].



(Trigger Event timeline added to original diagram)

Fig. 20 Phosphorus Increase Ratio, Lake Chetec, after 1968 Trigger Event (Garrison, P.J., LaLiberte, G.D., 2010)

Fig. 21 shows phosphorus concentrations that have “increased by a factor of 10 starting from 1950” [17]. If the phosphorus concentrations are referred to the Trigger Event timeline, it is possible that the major peaks in phosphorus after 1968 may have been due to the Trigger Event contamination, as the Rolling Thunder campaign commenced in 1965.

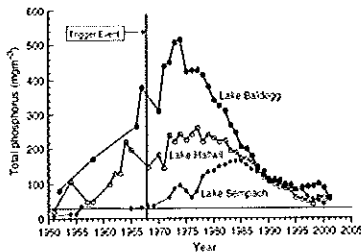


Figure 1. Total phosphorus concentration during spring circulation in Lake Saupach, Lake Baldegg and Lake Hallwil fresh-water after Stadelmann *et al.* (2002). The horizontal line indicates the critical phosphorus concentration to limit algal growth (30 µg P m<sup>-3</sup>).

(Trigger Event timeline added to original diagram)

Fig. 21 Phosphorus Increase Lake Baldegg, Lake Hallwil, and Lake Sampach, after the 1968 Trigger Event (Muller, R., Stadelmann P., 2004)

Fig. 22 shows the increase in phosphorus and fish yield in Lake Victoria after the 1968 Trigger Event. Note increase from 1965, as the Rolling Thunder campaign commenced in 1965.

The rapid increase in P concentrations at the V96-5MC core is not evident at the shallower 103 or the inshore Itome cores, and it occurs as a dramatic and quick onset after a prolonged period, after 1950, of steadily rising P concentrations in all three cores. Verschuren *et al.* (2002) used

oxygen sensitivities of chironomids that leave identifiable head capsules in lake sediments to reconstruct a chronology of the deoxygenation of the deep water. A steady decline in oxygen concentrations was observed at the V96-5MC site beginning about 1960 and stabilising at minimum inferred oxygen concentrations by the late 1970s. By the 1990s, the deep waters below 40 m were enduring prolonged seasonal anoxia (Hecky *et al.*, 1994). We hypothesise that the rapid increase in sedimentary P at V96-5MC resulted from a substantial increase in the availability of P liberated from internal sedimentary sources under increasingly prolonged anoxia. This apparently rapid rise in internal P loading recorded at V96-5MC stimulated inshore productivity as recorded in the Itome d13C and biogenic Si stratigraphies. Much of this increased productivity was likely accomplished by N-fixing cyanobacteria that were able to overcome increasingly severe N limitation. (Hecky, R.E., 2010) [18].

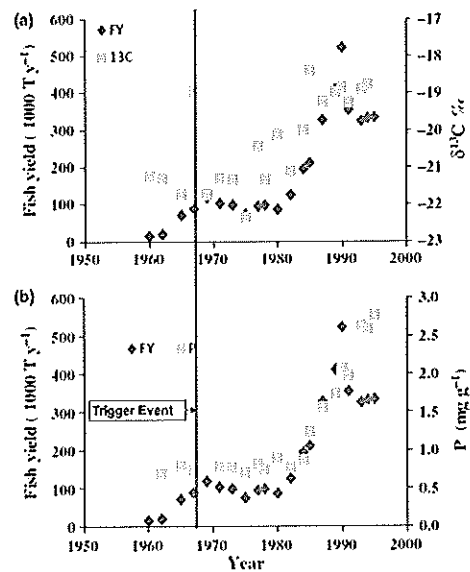


Fig. 11 (a) Temporal relationship between  $\delta^{13}\text{C}$  signature of sedimentary organic matter (Suess corrected) at Itome site and recorded total fish catches on Lake Victoria. (b) Temporal relationship between TP content of dated sediments at V96-5MC and recorded total fish catches of Lake Victoria. TP, total phosphorus.

(Trigger Event timeline added to original diagram)

Fig. 22 Phosphorus and Fish Yield Increase, Lake Victoria, after the 1968 Trigger Event (Hecky, R.E., Mugidde, R., Ramal, P.S., Talbot, M.R., Kling, G.W., 2010).

### A. Relationship of Phosphorus Dynamics of Main commercial fish Catches

If the Trigger Events of 1916 and 1968 are true then there should be Global observations of change where the introduction of significant phosphorus to the atmosphere, and subsequent deposition, would be expected to cause change in the ecosystem such as shown for Lake Victoria.

Changes in fish stock reproduction would be an indication of phosphorus change. Reference [15] described phosphorus pollution of Lake Geneva from 1959 to 2000 and expansion of bio systems as a result. Although there is a loose association between fresh water phosphorus pollution and the open Oceans, the Lake Geneva records can be used as a base reference to compare the advent of phosphorus pollution in the open Oceans and resultant side effects.

If reasonable correlations of phosphorus side effects are shown between the fresh water lake of Lake Geneva, and the open Oceans,

then it could be postulated that global phosphorus contamination occurred in 1968.

Fig. 23 shows the correlation of synchronism of catch fluctuations of "zonal-dependent" main commercial species [19]. In this group it can be seen that there is good correlation between the 1916 and the 1968 Trigger vents, in that only precisely after those events did the species increase in quantity and in synchronism. There was an initial precise synchronism in increase in fish stocks and then a precise synchronism in decline.

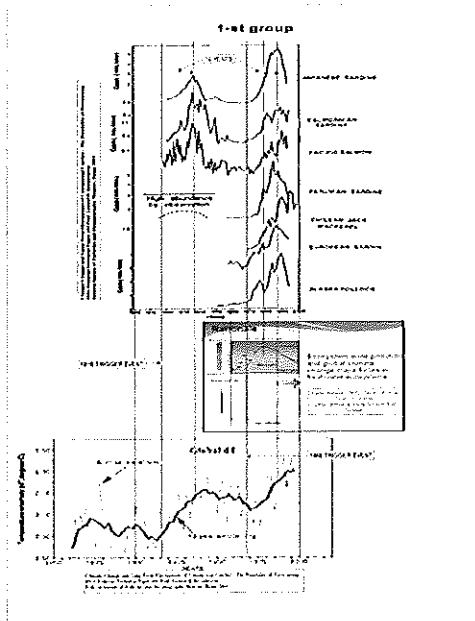


Fig. 23 Synchronous catch fluctuations of "zonal-dependent" main commercial species (Klyashtorin, B., 2001).

Both the 1916 and the 1968 events reached a precise synchronism of peak catch nineteen years after the occurrence of the Trigger Events. There is close correlation to Lake Geneva phosphorus pollution characteristic curve, indicating that for these species, an increase in phosphorus caused an increase in reproduction, with reproduction rate decreasing as the phosphorus load decreased over time.

Fig. 24 shows the correlation of synchronism of catch fluctuations of "meridional-dependent" main commercial species [19]. In this group it can be seen that there is good correlation between the 1916 and the 1968 Trigger Events, in that only precisely after those events did the species decrease in quantity and in synchronism. There was an initial precise synchronism in decrease in fish stocks and then a precise synchronism in increase. Both the 1916 and the 1968 events exhibited a precise synchronism of decline in catch after the occurrence of the Trigger Events. There is very close correlation to Lake Geneva phosphorus pollution characteristic curve, indicating that for these species, an increase in phosphorus caused a decrease in reproduction, with reproduction rate increasing as the phosphorus load decreased over time. Immediately and precisely at the 1968 Trigger Event, the fish stocks declined, indicating that the 1968 Trigger Event was the prime cause.

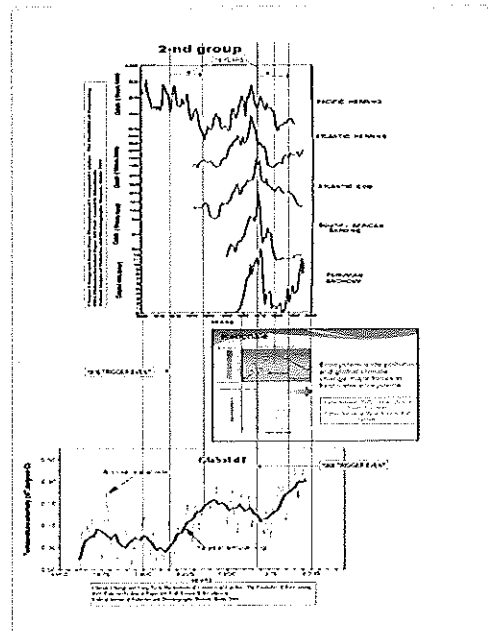


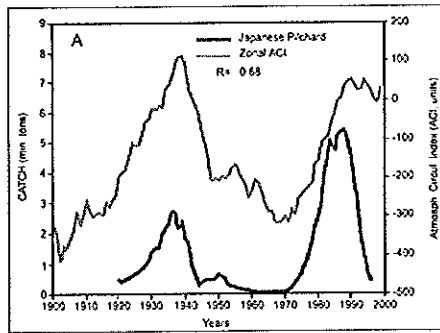
Fig. 24 Synchronous catch Fluctuations of "meridional-dependent" main commercial species (Klyashtorin, B., 2001).

It may be argued that the change in global temperature caused the variation in fish stock in Fig. 23 and Fig. 24. In Fig. 23 the Global temperature continues to increase but the fish growth rate decreases after a period and the temperature has no correlation to fish stock change thereafter. In Fig. 24 the Global temperature continues to increase but the fish growth rate initially decreases rapidly, then increases, and the temperature has no correlation to fish stock change thereafter.

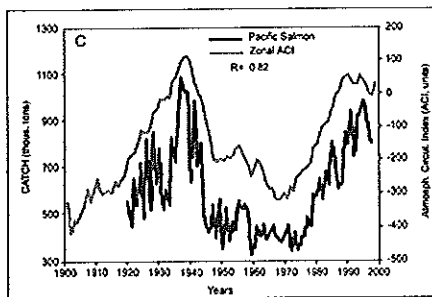
It is hypothesised that the species in Group 1, or their food chain, reacted positive to phosphorus increase. For a 19 year period post the Trigger Events of 1916 and 1968, fish stocks increased, and then decreased with precise correlation across most species, with the exception of a few species that kept increasing after the 1968 event. After the increase pulse due to the 1916 event, the fish stocks returned to a stable base level before the onset of the 1968 event. The fish stock increase and subsequent decline after the 1968 event could be due to the amount of residual phosphorus.

Group 2 or their food chain reacted negative to phosphorus increase. For a 19 year period post the Trigger Event of 1916 the fish stocks decreased, then increased with precise correlation across most species after the decrease caused by the 1916 event until 1968. There is exact correlation to the 1968 Trigger Event causing revision of fish stock to decline rapidly.

Reference [21] also describes the close correlation of the atmospheric circulation index (ACI) and the change in fish catch. One could form the conclusion that the ACI was the cause of the fish catch variability, however it has been shown that the Trigger Event, at least for the 1968 event, resulted in significant increase in rainfall and therefore significant increase in Latent Heat dissipation to the atmosphere. It is reasonable therefore to consider that the ACI index variation is not a recurring oscillation, but individual positive slope increases as a result of the 1916 and 1968 Trigger Events, as the ACI increases conform precisely to the Global temperature increase (dT), which in itself was most likely caused by the increase of Latent Heat dissipation in the atmosphere by increased rainfall as a result of the 1916 and 1968 Trigger Event.



(a)



(b)

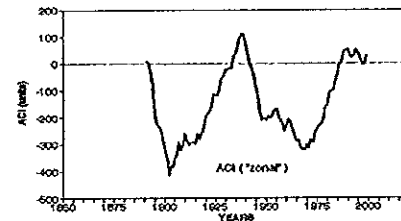
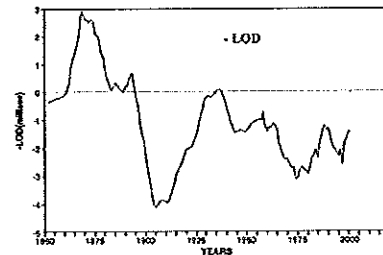
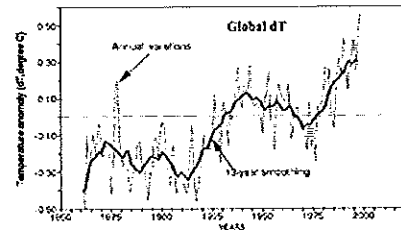
Fig. 25 Annual catch of Japanese pilchard and Pacific salmon in relation to the zonal atmospheric circulation index (ACI) (Klyashtorin, B., 2001).

Reference [19] describes the relationship between the length of day (LOD) of the Earth, the  $dT$  and the ACI. Increased Latent Heat from the Trigger Event rainfall increase would have increased the Equator-Pole Temperature Meridional Gradient, effecting the ACI and the LOD.

Where the characteristics of the atmospheric pressure fields "circulation epochs" have been considered as natural oscillation events, the characteristics as shown in Fig. 25 and Fig. 26 for the period 1915 to 1949 and 1968 to 2000 for  $dT$ , LOD and ACI could all have been a result of increased atmospheric heating by the Trigger Event increased rainfall Latent Heat of precipitation, creating individual positive slope events.

Similarity between the -LOD and  $dT$  dynamics makes it possible to assume the existence of some common factors inducing and controlling the observable synchrony in geophysical (LOD) and climatic ( $dT$ ) indices variation. The atmospheric circulation as a whole is strongly driven by the Equator-Pole Temperature Meridional Gradient. Greater warming in the polar region weakens this gradient in the lower troposphere, which leads to a general weakening of surface winds (Lambeck 1980).

The long-term dynamics of the atmospheric pressure fields over the Northern hemisphere during the last 90 years are characterised by the alternation of approximate 30-year periods ("circulation epochs") with relative dominance of either zonal or meridional atmospheric circulation (Dzerdzeevski 1969; Girs 1971; Lamb 1972; Lambeck 1980). Klyashtorin, B., 2001 [19].



Atmospheric Circulation Index (zonal ACI), 1891-1999

Fig. 26 The dynamics of the global air-surface temperature anomaly ( $dT$ ), 1861-1998, the negative Length of Day (-LOD), 1850-1998 and the ACI "zonal" (Klyashtorin, B., 2001).

The Food and Agriculture Organisation (FAO) of the United Nations, produced a comprehensive review of the state of world marine fishery resources [20].

If large increase or decrease in fish stocks are shown it would imply that the nutrient factors, and change in the food chain, rather than temperature alone, would have been responsible for high increases or decreases in the marine ecosystem. Phosphorus is essential to life, and in the marine environment, low or high phosphorus can alter the entire ecosystem, causing an imbalance in the food chain and oxygen depletion, leading to decline of some species against the gain of others.

Data pertaining to fish stock harvested showed significant variation in fish species from 1950 to 2000. There are many influences such as modern trawling techniques introduced in the 1960's, fish management and exclusion zones, and variations attributed to Global Warming.

If the Total Phosphorus load curve for the freshwater lake of Lake Geneva, is taken as a standard reference for possible phosphorus contamination of the Oceans, variations of fish stock harvest, species growth and species decline, can be correlated to the phosphorus contamination. If only a few instances showed correlation, it would be difficult to argue Global phosphorus contamination; however the review shows direct correlation over numerous locations across the Globe.

It is accepted that over-harvesting can cause serious decline in fish species, however the review shows that both the decline and the growth of species and harvesting occurred precisely to a timeline when the phosphorus was increasing, and then to when it peaked, and decreased back to normal.

There is also a cause and effect where mechanised and increased fishing can cause decline in species, where the proliferation of a species growth causes increase in fishing, or where the decline in species ecosystem causes decline in fishing. In particular there are examples where one species increase substantially as a result of the phosphorus timeline, and another species in the same habitat declines substantially.

It is not possible to determine what was the leading cause in many of these events, but the correlation to the phosphorus timeline and characteristic curve across the Globe is reasonable proof that global phosphorus contamination occurred from 1965-1968. The FAO report covered over 300 fish species. Fig. 28 represents a sample of the some 70 Figures produced by the Food and Agriculture Organization of the United Nations review of the state of the World marine fishery resources in 2005.

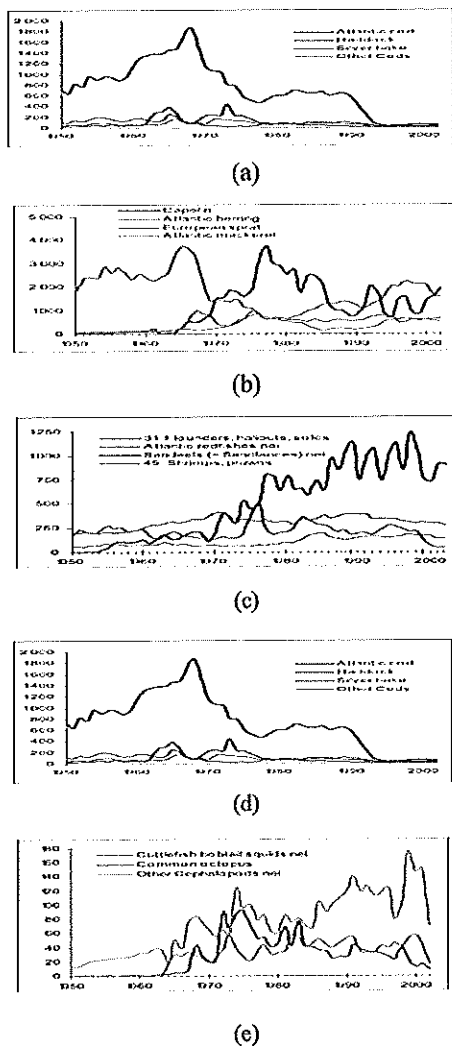


Fig. 28 Sample fish stock graphs (a) – (e), Food and Agriculture Organisation (FAO) of the United Nations, 2005, state of world marine fishery resources.

A number of research papers which have documented phosphorus since 1950 will show high concentrations of phosphorus beginning precisely at 1965 -1968. These papers will generally attribute the high phosphorus loading to agricultural runoff contamination. This could be true, as agricultural phosphate use increased during the 1960's, but also so would have the land based phosphorus contamination as a result of the 1968 Trigger Event 1965-1968 Global atmospheric phosphorus contamination.

There are similarities of the phosphorus loading characteristics that are generally consistent Worldwide –

1. Phosphorus increase is shown to begin in 1965, then accelerate after 1968.
2. The phosphorus loading pulse centres nominally in 1980.
3. The phosphorus loading pulse decreases to a low level, but higher than pre 1960, by 2000.

This has been shown in several of the preceding discussion references, but is perhaps best seen in Fig. 29, a study of the Irish Sea [21].

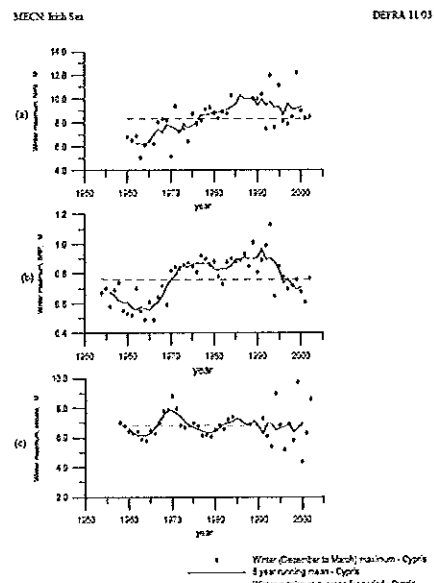


Figure 29 Winter maximum concentrations of nitrate, phosphate and silicate from the Celtic coast, East of Ireland.

Fig. 29 Phosphorus Levels in the Irish Sea Evens, G.L., Hardman-Mountford, N. J., Hartnoll, R.G., Hennington, K., Mitchelson-Jacob, E.G., Shammon, T., and Williams, P.J. le B., (2003)

If Fig. 29 (b) is expanded as in Fig. 30, the precision of the phosphorus timeline to the 1965 to 1968 Rolling Thunder Campaign in Vietnam is shown.

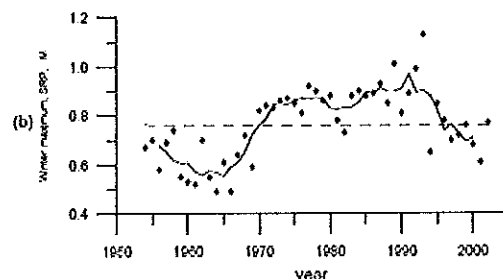


Fig. 30 Irish Sea Phosphorus Timeline

The repeatability of this curve across multi disciplines and across Global locations is reasonable evidence that phosphorus loading on land or marine environments occurred as a result of atmospheric phosphorus contamination from 1965 to 1968 as a result of the Rolling Thunder Campaign in Vietnam.

If the level of phosphorus was significant enough to have changed phosphorus loading in nearly every location on Earth, it is reasonable evidence that the phosphorous contamination of the atmosphere would have been responsible for the high rainfall events of the 1968 Trigger Event as previously described.

#### X. OTHER WHITE PHOSPHORUS USE

There is reported evidence that white phosphorus was introduced in 1916 in World War I [12]. The Australian Cumulative Rainfall Anomaly shows in Fig. 8 that there was initiated at 1916, an increase in rainfall event. Other data, such as the North Carolina extraordinary rainfall events as shown in Fig. 31, correlate to a high rainfall event in 1916 [22].

Global Mean Temperature data, as in Fig. 31, indicates that there may have been an initiation of a 'Trigger Event' at circa 1940 [6]; however other data as in Fig. 44 shows that the Atmospheric Atomic bomb tests from 1940 to 1963 disrupted the World's Simple Harmonic Motion of weather, preventing the onset of an oscillation as described for the Trigger Event at circa 1940.

#### XI. WEATHER MODIFICATION PROGRAM – VIETNAM

Between 1967 and 1972 the United States conducted specific rain seeding operations in Vietnam in order to increase normal monsoon rainfall. 2,602 air sorties delivered 47,409 units of silver and lead iodide to the atmosphere over Vietnam [23]. The Top Secret United States Senate Subcommittee in 1974 recorded details of this program, including outcomes. It is possible that this program contributed to, or was, the main Trigger Event, as the timeline is the same for the use of phosphorus bombs in Vietnam.

The report details that the program was only conducted during still weather conditions in order to be effective, thereby minimising the possibility of wide distribution of iodide into the atmosphere.

It is evident by the Global rainfall data that the 1968 Trigger Event occurred globally, inferring significant and widespread atmospheric contamination, requiring substantial quantities of contaminate, such as the extreme quantity of aggressive hygroscopic phosphorus pentoxide aerosol.

#### XII. TRIGGER EVENT CORRELATION TO WORLD TEMPERATURE ANOMALY

The correlation of the Trigger Event to the Global temperature increase can be seen in Fig. 31 [23]. The Global temperature increase since 1900 has been in two discrete periods, 1916 to 1940, and 1970 to 2010. Both these periods correspond precisely to the 1916 and the 1968 White Phosphorus events. The temperature increase from 1916 to 2010 constitute all temperature increase associated with Global Warming.

The extraordinary high rainfall events of North Carolina precisely correspond to White Phosphorus events [22].

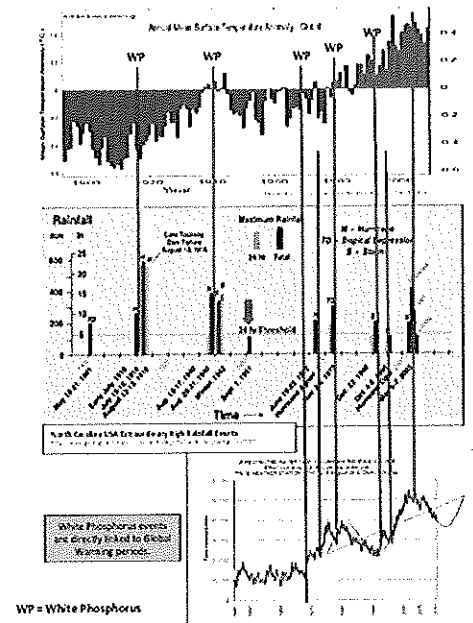


Fig. 31 Annual Mean Temperature Anomaly – Global

The correlation of the Trigger Event to the Australian temperature increase can be seen in Fig. 32 [7]. The Australian temperature increase since 1900 has occurred precisely since the 1968 Trigger Event.

The extraordinary high rainfall events of North Carolina precisely correspond to White Phosphorus events [22]. In Australia the temperature increase periods after 1968 can be seen to be more precisely associated with the White Phosphorus events.

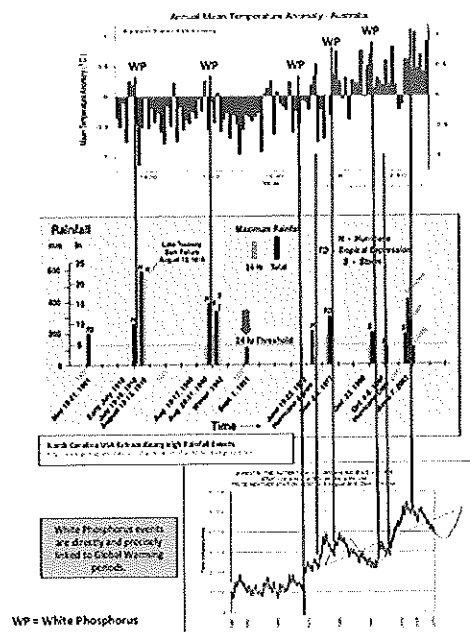


Fig. 32 Annual Mean Temperature Anomaly – Australia



The correlation of the Trigger Event at 1968 to increases in temperature rise of the Surface and the Lower Troposphere is shown in Fig.33 [25]. The variations in temperature of the atmospheric layers only commenced after the 1968 Trigger Event and have a temperature increase across the same time frame as the mean rainfall increase.

The Agung, El Chichon, and the Pinatubo atmospheric periods perfectly align with the sine oscillation phases of the Trigger Event rainfall sine wave oscillation.

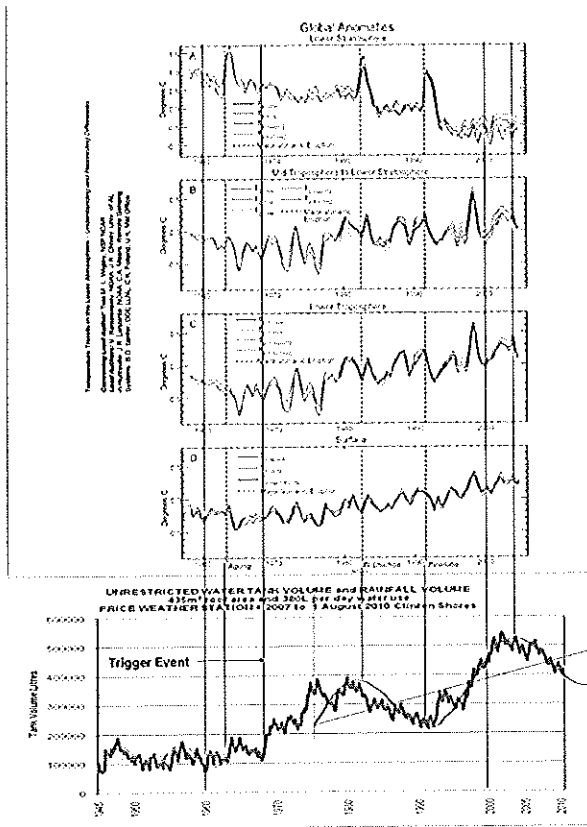


Fig. 33 Atmospheric Temperature Global Anomalies (Wigley et al, 2006, pg 8)

The correlation of the Trigger Event to the Hobart minimum temperature increase can be seen in Fig. 34 [24]. The extraordinary high rainfall events of North Carolina precisely correspond to Hobart minimum temperature increase events [22]. The temperature increase periods can be seen to be precisely associated with the Trigger Event White Phosphorus events.

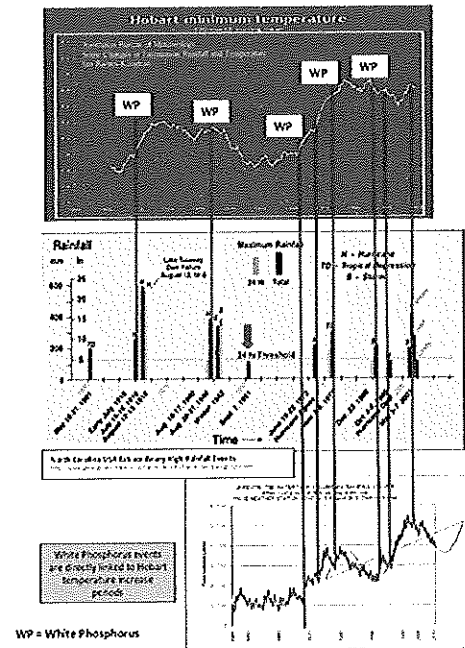


Fig. 34 Hobart Minimum Temperature

### XIII. PACIFIC DECADAL OSCILLATION

Much speculation has existed about the Pacific Decadal Oscillation. It was best expressed by Donald R. Mock, NOAA-Skaggs Laboratory Director in 1981, where he stated:

“From the exhaustive correlation studies of Walker in the 1920's to the 1980 Kelvin wave-front theories of Wyrski and others, the phenomenon known as the Southern Oscillation has attracted the considerable interest of many capable meteorologists and oceanographers, yet a comprehensive explanation of the observed characteristics has not yet been obtainable” [26].

Since that time often extremely complex explanations have emerged. Fig. 35 shows the precise correlation of the Pacific Decadal Oscillation to the 1916 and the 1968 Trigger Events [27]. The period P1 is a delay time to the onset of a significant positive Pacific Decadal Oscillation index from the 1968 Trigger Event. The Pacific Decadal Oscillation index existed in a significant positive period (P2) until precisely the Price Cumulative Rainfall oscillation passed through zero crossing as it entered the second sine cycle. P3 and P4 are shown in the same time frames as P1 and P2, indicating that in 1916 a similar event as that of 1968 occurred to initiate the PDO oscillation.

It could be hypothesised that the PDO caused the Price Rainfall Anomaly oscillation, however the 1968 and the 1916 events document use of white phosphorus, and the similarity of the P1, P3 and the P2, P4 periods after the trigger events of 1916 and 1968, and the precise correlation of the Rolling Thunder white phosphorus use to the initiation of the 1968 Trigger Event create a strong hypothesis that the Pacific Decal Oscillation is actually a result of the 1916 and the 1968 Trigger Events.

Atmospheric Atomic Bomb tests, conducted between 1946 and 1963, are reflected in the variation to the Pacific Decadal Oscillation during that period.

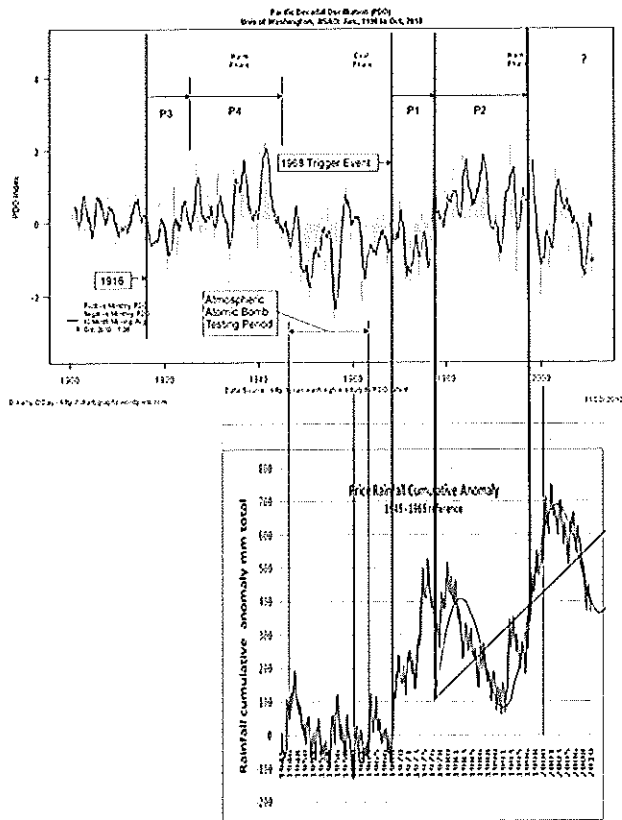


Fig. 35 Pacific Decadal Oscillation (University of Washington JISAO, 2010)

#### XIV. ATMOSPHERIC CARBON DIOXIDE INCREASE

Fig. 36 shows the increase in Atmospheric Carbon Dioxide from 1960 to 2010 from the NOAA Earth System Research Laboratory at Mauna Loa [28].

Smoothing functions can often make trends seem what they are not. In Fig. 35, the CO<sub>2</sub> increase may seem to be progressing along an ever increasing non linear function, however, if best fit straight line functions are superimposed, it can be seen for the period between 1960 and 2010 that the CO<sub>2</sub> increase has been progressing for the majority of the time along straight line functions, rather than having a continuum of non-linear increase.

Fig. 35 shows correlation of those increases to the Trigger Event rainfall oscillation. From just after 1968, continuing to circa 1974, there is an increase pulse in atmospheric CO<sub>2</sub>. This increase in CO<sub>2</sub> was most likely due to immediate CO<sub>2</sub> release due to the Trigger Event phosphorous pentoxide reactions such as CO<sub>2</sub> release from common Calcium Carbonate and phosphoric acid, a by-product of the White Phosphorus bombs ( $3Ca(CO_3) + 2H_3PO_4 \gg 3CO_2 + 3H_2O + Ca_3(PO_4)_2$ ).

Variations in CO<sub>2</sub> increase can be directly correlated to the sine wave phases of the Trigger Event. There are two phases corresponding to the negative slope of the sine wave where positive feedback is indicated. It is considered that during these phases that atmospheric moisture will be increasing in the atmosphere, leading

to increased rainfall as the sine curve progresses from the negative slope towards a change to the positive. The Price data is relative to South Australia.

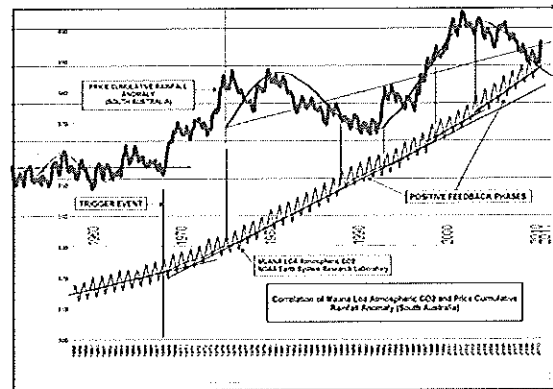


Fig. 36 Atmospheric Carbon Dioxide Increase Correlation to the Trigger Event (NOAA Earth System Research Laboratory, 2010)

Fig. 37 shows the relationship of the Mauna Loa carbon dioxide increase per annum rate and the Rainfall Cumulative Anomaly at Price in South Australia [28]. There is a direct relationship between the rate of increase of cumulative rainfall and the increase rate of Carbon Dioxide, with the rainfall anomaly leading change in Carbon Dioxide (data Y Axis scales adjusted to display data graphs to a common scale).

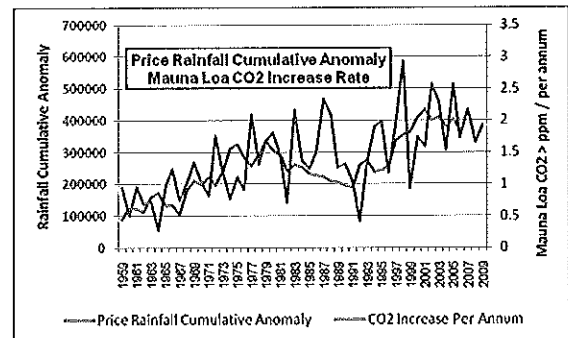


Fig. 37 Correlation of Rainfall Cumulative Anomaly and Carbon Dioxide Rate of Increase (NOAA Earth System Research Laboratory, 2010)

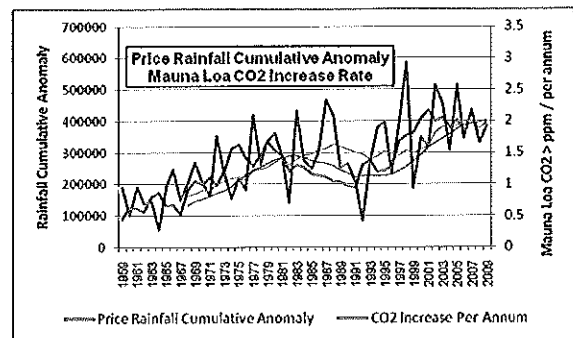


Fig. 38 Phase Relationship between Rainfall Cumulative Anomaly and Carbon Dioxide Rate of Increase with Ten Year Running Average Trend Lines (NOAA Earth System Research Laboratory, 2010)

In Fig. 39 the correlation of the Excel generated linear trend lines for both the Price Rainfall Cumulative Anomaly and the Mauna Loa Carbon Dioxide increase per annum increase rate show the same rate of mean increase from 1959 to 2009 (data Y Axis scales adjusted to display data graphs to a common scale).

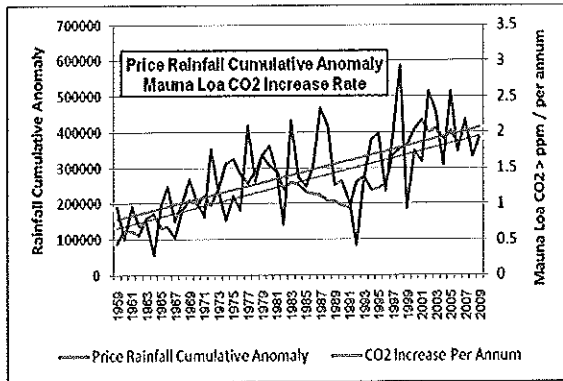


Fig. 39 Correlation of Rate of Increase of Linear Trend Lines of Rainfall Cumulative Anomaly and Carbon Dioxide Rate of Increase (NOAA Earth System Research Laboratory, 2010)

It can reasonably be concluded that the Rainfall Cumulative Anomaly preceded and caused change in the Carbon Dioxide increase, with a decrease lag, and an increase lag between rainfall anomaly change and Carbon Dioxide change.

Fig. 40 shows that the association of sustained Cumulative Rainfall Anomaly and Carbon Dioxide (CO<sub>2</sub>) increase can be explained by changes in ecology systems such as microbial mediated Carbon Dioxide evolution from dead vegetative matter, where research has shown that release of CO<sub>2</sub> from dead plant matter is directly linked to moisture availability. The dead plant matter increased CO<sub>2</sub> evolution at a 30 fold increase when moisture was available, compared to a dry state [29]. The increase in Rainfall Cumulative Anomaly would have resulted in a global increase in microbial mediated Carbon Dioxide.

This is consistent with the phase lag relationship of Rainfall Cumulative Anomaly and Carbon Dioxide rate of change as shown in Fig. 38. The rate of change of the rainfall between the decrease of rainfall during the negative sine slope and the increase in rainfall as per the Price Rainfall Cumulative Anomaly characteristic of Fig. 38 would have resulted in a slow decrease lag in microbial mediated Carbon Dioxide evolution, but an accelerated increase lag due to a more rapid increase in rainfall at the commencement of the positive sine slope.

Fig. 41 shows the direct correlation of Australian Rainfall Cumulative Anomaly increase, the Australian Temperature Anomaly increase, and atmospheric Carbon Dioxide increase [3],[6],[28]. The Australian Rainfall Cumulative Anomaly increase coincides with the intersection of straight line function increases of Carbon Dioxide, and the increase in Carbon Dioxide rate at 1972. Fig. 41 shows that from 1972 to 2010 variations in CO<sub>2</sub> precisely correlate to the variations of level of sustained Australian Rainfall Cumulative Anomaly. The Australian Temperature Anomaly increase coincides with the beginning of escalation of Carbon Dioxide increase at 1972, and the specific increase of Carbon Dioxide associated with the Trigger Event White Phosphorus Trigger Event at 1968.

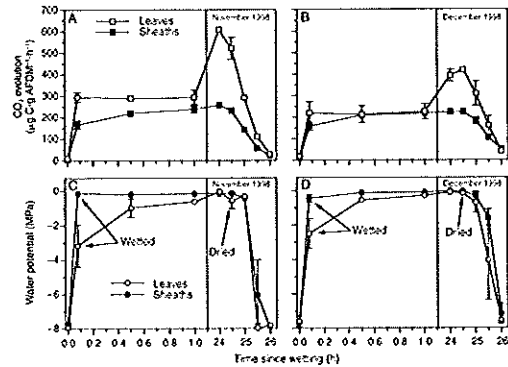


Fig. 40 CO<sub>2</sub> Evolution Increase from Wetted Plant-Litter (Kuehn, K.A., Steiner, D., and Gessner, M.O.,2004)

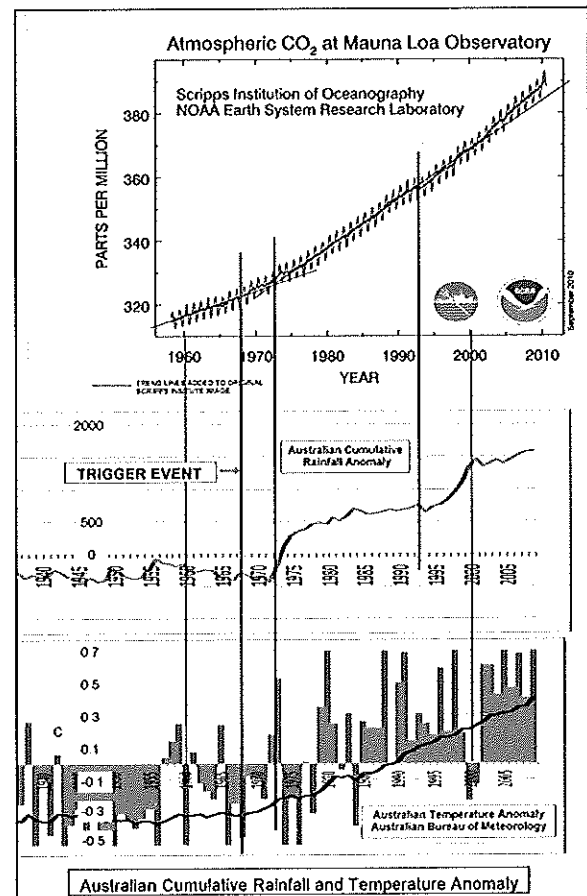


Fig. 41 Correlation of Carbon Dioxide Increase to Australian Rainfall Cumulative Anomaly and Temperature Anomaly

## XV. RAINFALL PREDICTION

The Trigger Event and subsequent rainfall oscillation as per Fig. 2 has resulted in a new understanding of rainfall and weather.

The concept of using progressive addition to create a cumulative anomaly characteristic has resulted in the ability to not only better understand how World weather works as part of Simple Harmonic oscillation, but to have the capability of being able to forecast rainfall trend and variation well into the future with a high degree of confidence. The cumulative anomaly characteristics produce well defined trajectory paths that can predict rainfall well into the future. Because the trajectory paths are following mathematical harmonic characteristics, it is possible to calculate what rainfall will be necessary to obtain the future results.

Fig. 42 shows the variation of a sample of South Australian Weather Station rainfall characteristics compared to the Trigger Event of 1968 as Cumulative Rainfall Anomaly 'water tank' volumes with a starting volume of 100,000L, a collection area off 435m<sup>2</sup> and a daily water use of 380L. Data for the Cumulative Rainfall Anomalies shown were derived from the Bureau of Meteorology rainfall data for each location [30]-[33].

It can be seen that although all locations responded to the first high rainfall oscillation of the Trigger Event, thereafter, significant variations in rainfall occurred at differing locations, even though some locations are only a few kilometres apart.

These variations produce the characteristics of the South Australian and Australian rainfall anomalies as per Figs. 5-8.

The Trigger Event and subsequent rainfall oscillation to 2010 caused some locations to increase rainfall, while others to seriously decrease rainfall. Generally, the lower rainfall locations increased rainfall, while the higher rainfall locations decreased rainfall, as per the characteristics of the Clare location in Fig. 42.

Such changes in rainfall have led to the belief that since the year 2000 in particular, 'Global Warming' has caused serious decline in rainfall, when in fact there has been primarily changes in the oscillation dynamics of rainfall between different locations.

While the trajectories of rainfall in the locations shown in Fig. 42 may seem random, they are not. Each is following a path determined by a mathematical function. The trajectory will be a vector result of the interaction of Simple Harmonic Motion oscillation of the World weather system relative to the local area.

Significant differences between rainfall characteristics are found between locations often a few kilometres from each other, in similar geographic areas. Some locations that have specific geographical location such as Clare shown in Fig. 42, exhibit what at first appears to be no connection to other locations, but Fig. 42 shows that it is indeed directly linked to the characteristics of the Trigger Event, as significant change occurred after the Trigger Event of 1968.

The results of Fig. 42 would be obtained in a situation where multiple oscillation mode areas exist within an oscillation, a common and expected occurrence in any engineering oscillation situation. Although treated in the past as individual locations with random rainfall characteristics at any one time, Fig. 42 shows that all locations are mathematically linked when viewing the long term Cumulative Rainfall Anomaly. Changes in rainfall oscillation frequency will cause changes in mode area oscillation, and subsequent changes in rainfall.

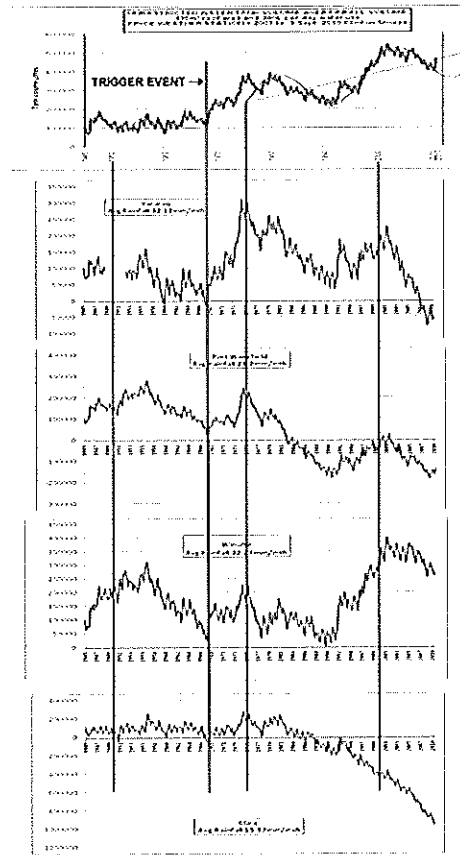


Fig. 42 Variation in South Australian Weather Station Cumulative Rainfall Anomaly Characteristics (Australian Bureau of Meteorology, 2010)

Fig. 43 shows the weather stations of Fig. 42 plotted on the same graph. It is clear that prior to 1968, all stations were in reasonable unison with weather variation. Precisely at 1968, the rainfall at the weather stations departs from the prior unison, with some gaining rainfall, while others seriously declined. There is a common misconception that since circa 2000 there has been a serious decline in rainfall due to Global Warming, but in fact is part of an oscillation cycle, that by October 2020 has already began to move into a period of increasing rainfall (Price weather station). Any repeating, non-sinusoidal waveform consists of a series of sinusoidal waveforms of different amplitudes and frequencies added together. The Trigger Event consisted of a bootstrap event that excited the Global weather oscillation into a new series of frequencies and resulting sub harmonic and mode points. The weather stations in Fig. 42 are within a few hundred kilometres of each other, indicating that the variation in rainfall between regions is not due to an overall Australian or Global change, but localised harmonic mode point changes in weather conditions. This is confirmed by Fig. 6 that showed that South Australia had an overall increase in rainfall anomaly when all South Australian weather stations were combined. There is the expectation in such a scenario that some locations such as Clare that had prior to 1968 experienced consistent high rainfall, may enter an oscillation mode that seriously reduces rainfall as a result of the Trigger Event.

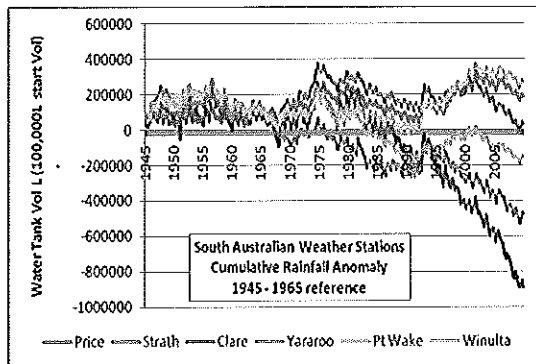


Fig. 43 Trigger Event Effect on Weather Station Cumulative Rainfall Anomaly (Australian Bureau of Meteorology, 2010)

Although Global weather oscillation and mode is well known, the effect on localised weather within a few kilometre range has been underestimated.

Fig. 44 shows the relationship of the phases of oscillation between weather station locations in South Australia, for yearly rainfall. Rainfall graph data provided by Thomson (2010, pers. comm, 10 June 2010) shows that at precisely 1916 there exists for the South Australian weather stations shown, a simultaneous increase in rainfall, altering the previous rainfall oscillation frequency cycle by initiation of a rapid increase in rainfall at all stations simultaneously.

The synchronous oscillations at all weather stations continue until circa 1935 - 1940. From 1940 to 1968 many weather stations exhibit non synchronised rainfall data. After 1963 synchronism of rainfall data started to recommence. Atmospheric Atomic bomb testing was conducted from 1946 to 1963. At 1968, all stations are again synchronised in oscillation after the Trigger Event.

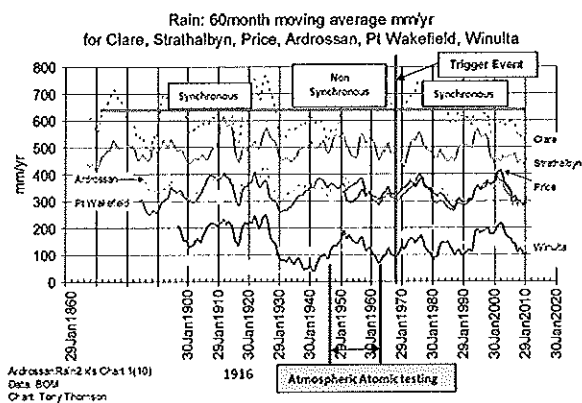


Fig. 44 Five Year Trend Line Rainfall Oscillation Phases (Thompson, T, 2010)

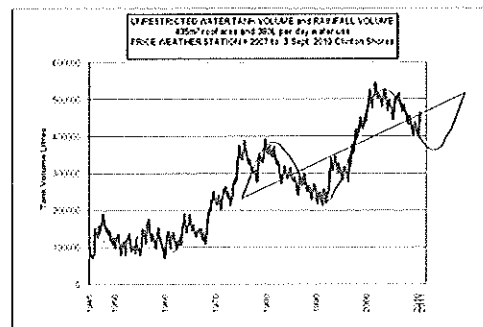
Using the Cumulative Rainfall Anomaly characteristic, it is possible to accurately predict rainfall variations a decade ahead with a high degree of confidence. Rainfall can be predicted with such accuracy that the monthly rainfall in mm can be reasonably accurately known years, if not decades ahead.

Traditional prediction, based on historical knowledge of weather patterns and probability, is variable. The cumulative rainfall anomaly gives a smooth trajectory that enables accurate prediction many years ahead by simply doing a reverse calculation to that which would have created the cumulative anomaly at any future point.

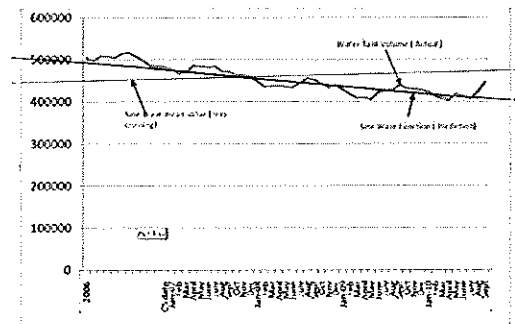
Price rainfall, as shown in Fig. 45, is following a precise sine curve that allows for a very high degree of accuracy. By expanding the sine wave function, it has been possible to accurately predict rainfall since 2006 at Clinton Shores. The sine wave prediction line was established in 2006.

As predicted, as the sine curve reaches the lower half of the negative sine wave swing, rainfall will increase significantly in order to alter the rainfall trajectory from a negative slope to a positive slope. This will result in substantial rainfall events and associated severe weather conditions.

If the rainfall, as it is in 2010, becomes more positive than the anticipated trajectory, it indicates that positive feedback of energy is occurring.



(a)



(b)

Fig. 45 Accurate Rainfall Predictions along Known Sine Function Curve.

Fig. 46 shows the correlation of the sine oscillation and the Southern Oscillation Index for 2006 to the end of 2010 [35]. It can be seen that as the oscillation nears the bottom of the negative sine swing, requiring a rapid acceleration in rate of rainfall in order to change the cumulative rainfall anomaly from a negative slope to a positive one in order to follow the sine wave function, the Southern Oscillation Index becomes more positive in a non linear manner.

The anticipated result is for the Southern Oscillation Index to continue to become more positive until 2012-16, with associated increased rainfall and weather events.

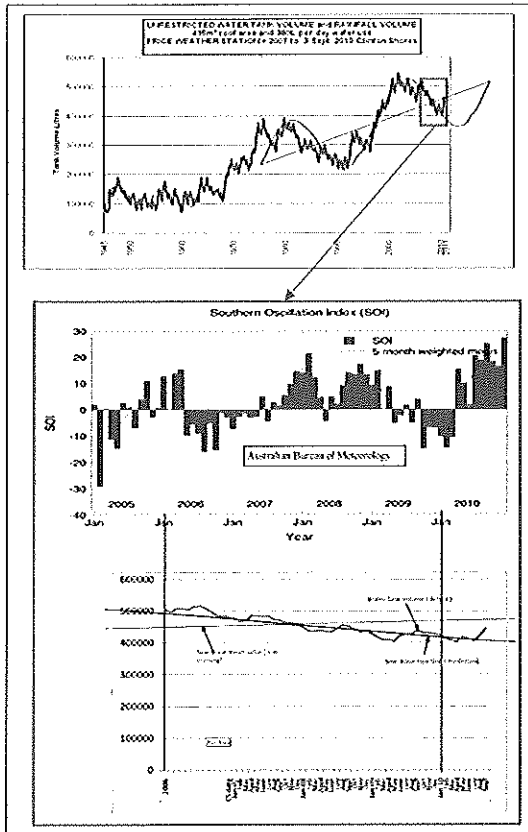


Fig. 46 Southern Oscillation Index Correlation to the Sine Oscillation.

The World high rainfall and weather events of latter 2010 and early 2011 were accurately predicted to occur in 2006 using the oscillation sine curve projection curve as in Fig. 45 and Fig. 46.

In latter 2010 and 2011 severe floods and cyclone activity in Queensland, Australia caused significant damage. Fig. 47 shows the relationship of the Queensland floods and cyclones to the Cumulative Rainfall Anomaly oscillation characteristic. It can be seen that during the rainfall sine oscillation, there is little extraordinary rainfall or weather activity during the positive anomaly slope of the sine curve. As the sine curve begins the downward negative slope, weather activity increases, with the majority of severe weather occurring during the period of maximum rate of change in the Cumulative Rainfall Anomaly oscillation as it transitions from a negative slope to a positive slope at the lower section of the negative cycle.

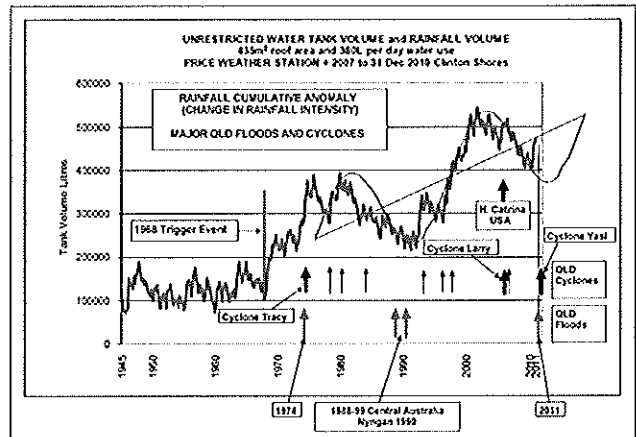


Fig. 47 Correlation of Severe Queensland, Australia, Floods and Cyclones

For reference, Hurricane Katrina, USA, and Cyclone Tracy, Darwin, Australia are shown. Cyclone Tracy, which destroyed the City of Darwin on Xmas Day 1974, occurred during the initial Trigger Event effect on rainfall and weather. Hurricane Agnes occurred in the USA in 1975 (see North Carolina data Fig. 31).

The weather events that have occurred globally during the period of the negative sine cycle of the Cumulative Rainfall Anomaly during the second oscillation phase have increased in intensity significantly to previous known weather events.

The periods of extreme weather in the form of drought, flood and extreme weather events are accurately predictable.

## XVI. CONCLUSIONS

[20] Phosphorus pollution of the Earth atmosphere occurred between 1965 and 1968.

- [1] In 1968 a Trigger Event caused a significant change to the simple harmonic motion of World Weather resulting in increased rainfall and global temperature increase through Latent Heat release.
- [2] The 1968 Trigger Event was due to atmospheric contamination of hygroscopic phosphorus pentoxide as a result of the use of white phosphorus bombs during the Vietnam Rolling Thunder campaign.
- [3] The 1968 Trigger Event caused severe changes in rainfall by initiation of Simple Harmonic Motion sine wave oscillation.
- [4] There is reasonable evidence that a Trigger Event in 1916 as a result of World War 1, caused an increase in rainfall and global temperature increase through Latent Heat release.
- [5] There is reasonable evidence that in circa 1940 as a result of World War 2, that a rainfall increase and temperature increase event occurred associated with white phosphorus bombs.
- [6] There is reasonable evidence that circa 1940 to 1963 Atmospheric Bomb testing effected the simple harmonic motion of World Weather, preventing rainfall oscillation from occurring.
- [7] Variation in the rainfall has distinct changes that precisely correlate to the 1968 Trigger Event.
- [8] Increase in Lower Troposphere and Surface temperature has distinct changes in variation that precisely correlate to the 1968 Trigger Event and increased rainfall.
- [9] Increase in atmospheric Carbon Dioxide associated with Global Warming has distinct changes in variation that precisely correlate to the Trigger Event and increased rainfall.
- [10] Increase rates of atmospheric Carbon Dioxide can be directly linked to increase of Carbon Dioxide emissions from microbial mediated Carbon Dioxide evolution from dead vegetative matter and increased Global moisture variation.
- [11] Phase relationship between Rainfall Cumulative Anomaly and Carbon Dioxide increase determine that the increase in Rainfall Cumulative Anomaly caused the increase in Carbon Dioxide through microbial mediated Carbon Dioxide evolution.
- [12] Increase in atmospheric Carbon Dioxide as a result of increased microbial mediated Carbon Dioxide evolution has contributed to Global Warming by Greenhouse Effect.
- [13] Global Warming positive feedback of rainfall oscillation energy is most likely occurring as a result of the Trigger Event simple harmonic motion rainfall oscillation cycle causing variations in Atmospheric Carbon Dioxide and water vapour.
- [14] There is evidence that Global Warming positive feedback of rainfall oscillation energy is increasing in magnitude.
- [15] From the onset of the Trigger Event in 1968 there is no evidence of extraordinary data variation in phase, magnitude, or time line relationship of Carbon Dioxide increase that can be attributed to post 1968 Anthropological 'Carbon Emissions'.
- [16] World temperature increases attributed to the 1916 WW1 event and the 1968 Trigger Event constitute all of the World temperature increase attributed to Global Warming.
- [17] The Pacific Decadal Oscillation is shown to be directly linked to the 1916 and the 1968 Trigger Events.
- [18] Rainfall variation in specific local areas may be due to weather oscillation modes.
- [19] Rainfall Cumulative Anomaly (Progressive Addition) enhances future rainfall prediction.

## XVII. ACKNOWLEDGMENT

Personal communication with Thomson T., Adelaide, South Australia, regarding rainfall characteristics.

## XVIII. REFERENCES

- [1] Clinton Shores, *A true water self sustainable residential development*, viewed 6 August 2010, <<http://www.clintonshores.com.au/>>.
- [2] Australian Bureau of Meteorology (2006), *PriceMonthlyrainfall.csv*, Australian Bureau of Meteorology, Adelaide South Australia.
- [3] Australian Bureau of Meteorology (2010a), *Australian climate variability & change - Time series graphs – Australian Rainfall Anomaly*, viewed 6 August 2010, <[http://www.bom.gov.au/cgi-bin/climate/change/timeseries.cgi?graph=rranom&area=aus&season=0112&ave\\_yr=0](http://www.bom.gov.au/cgi-bin/climate/change/timeseries.cgi?graph=rranom&area=aus&season=0112&ave_yr=0)>.
- [4] Australian Bureau of Meteorology (2010d), *Australian climate variability & change - Time series graphs – South Australian Rainfall Anomaly*, viewed 6 August 2010, <[http://www.bom.gov.au/cgi-bin/climate/change/timeseries.cgi?graph=rranom&area=sa&season=0112&ave\\_yr=0](http://www.bom.gov.au/cgi-bin/climate/change/timeseries.cgi?graph=rranom&area=sa&season=0112&ave_yr=0)>.
- [5] Climate4you (2009), *Normal climate and normal period*, viewed 1 October 2009, <<http://www.climate4you.com/NormalClimateNormalPeriod.htm>>.
- [6] Australian Bureau of Meteorology (2010b), *Australian climate variability & change - Time series graphs – Australian Mean Temperature Anomaly*, viewed 6 August 2010, <[http://www.bom.gov.au/cgi-bin/climate/change/timeseries.cgi?graph=tmean&area=aus&season=0112&ve\\_yr=0](http://www.bom.gov.au/cgi-bin/climate/change/timeseries.cgi?graph=tmean&area=aus&season=0112&ve_yr=0)>.
- [7] Australian Bureau of Meteorology (2010c), *Australian climate variability & change - Time series graphs – South Australian Mean Temperature Anomaly*, viewed 6 August 2010, <[http://www.bom.gov.au/cgi-bin/climate/change/timeseries.cgi?graph=tmean&area=sa&season=0112&ave\\_yr=0](http://www.bom.gov.au/cgi-bin/climate/change/timeseries.cgi?graph=tmean&area=sa&season=0112&ave_yr=0)>.
- [8] Kiehl, J.T. and Trenberth, K.E. (1997), *Earth's Annual Global Mean Energy Budget*, Bulletin of the American Meteorology Society, 78 (2), 206.
- [9] JRA-25 Atlas (2010), *Column climatologies – Annual Mean Column integrated heating*, viewed 6 August 2010, <[http://ds.data.jma.go.jp/gmd/jra/atlas/column-1/hatm\\_ANN.png](http://ds.data.jma.go.jp/gmd/jra/atlas/column-1/hatm_ANN.png)>.
- [10] Wikipedia (2010), *Greenhouse gas*, viewed 2 August 2010, <[http://en.wikipedia.org/wiki/Greenhouse\\_gas#Role\\_of\\_water\\_vapor](http://en.wikipedia.org/wiki/Greenhouse_gas#Role_of_water_vapor)>.
- [11] The History Place (2010), *The Vietnam War – The Jungle War 1965 - 1968*, viewed 2 August 2010, <<http://www.historyplace.com/unitedstates/vietnam/index-1965.html#thun>>.
- [12] AllExperts (2009), *White Phosphorus –Weapon*, viewed 1 October 2009, <[http://www.associatepublisher.com/e/w/wh/white\\_phosphorus\\_\(weapon\).htm](http://www.associatepublisher.com/e/w/wh/white_phosphorus_(weapon).htm)>.
- [13] ABC Catalyst (2009), *Cloud Seeding*, viewed 20 October 2009, <<http://www.abc.net.au/catalyst/stories/2714955.htm>>.
- [14] Sonic Bomb (2010), *Vietnam Bombing Run*, viewed 2 August 2010, <<http://www.sonicbomb.com/xv1.php?vid=vietnamb&id=624&s=28&w=560&h=420&ttitle=Vietnam%20Bombing%20Run>>.
- [15] Molinero, J.C. (2009), *Climate Effects on Pelagic Ecosystems*, Leibniz Institute of Marine Sciences. IFM-GEOMAR, Kiel, Germany.
- [16] Garrison, P.J., LaLiberte, G.D. (2010), *Paleoecological Study of Lake Chetek*, Sawyer County, Wisconsin Department of Natural Resources, Bureau of Science Services, Sawyer County.
- [17] Muller, R., Stadelmann P. (2004), *Fish habitat requirements as the basis for rehabilitation of eutrophic lakes by oxygenation*, Swiss Institute for Environmental Science and Technology (EAWAG), Kastanienbaum, Switzerland; Environmental Protection Agency of Canton Lucerne, Switzerland.
- [18] Hecky, R.E., Mugidde, R., Ramal, P.S., Talbot, M.R., Kling, G.W. (2010), *Multiple stressors cause rapid ecosystem change in Lake Victoria*, Large Lakes Observatory, University of Minnesota Duluth, Duluth, MN, U.S.A., Fisheries Resource Research Institute, Jinja, Uganda, Fisheries and Oceans Canada, Freshwater Institute, Winnipeg, MB, Canada, Geological Institute, University of Bergen, Bergen, Norway – Department of Ecology and Evolutionary Biology, University of Michigan, Ann Arbor, MI, U.S.A.
- [19] Klyashtorin, B., (2001), *Climate change and long term fluctuations of commercial catches*, Federal Institute of Fisheries and Oceanography Moscow, Rome.
- [20] Food and Agriculture Organisation of the United Nations (2005), *Review of the world marine fishery resources*, Marine Resources Service, Fishery Resources Division, FOA Fisheries Department, Rome.
- [21] Evens, G.L.<sup>1</sup>, Hardman-Mountford, N. J.<sup>3</sup>, Hartnoll, R.G.<sup>2</sup>, Hennington, K.<sup>2</sup>, Mitchelson-Jacob, E.G.<sup>1</sup>, Shammon, T.<sup>2</sup>, and Williams, P.J. le B.<sup>1</sup>, (2003), *Long-term environmental studies in the Irish Sea: a review*, 1. University of Wales, Bangor, School of Ocean Sciences, Menai Bridge, Anglesey LL59 5AB, 2. Port Erin Marine Laboratory, University of Liverpool, Port Erin, Isle of Man IM9 6JA, 3. Marine Biological Association, The Laboratory, Citadel Hill, Plymouth PL1 2PB.
- [22] North Carolina Geological Survey (2010), *Geologic hazards in North Carolina – Landslides*, viewed 2 August 2010, <[http://www.geology.enr.state.nc.us/Landslide\\_Info/Landslides\\_background.htm](http://www.geology.enr.state.nc.us/Landslide_Info/Landslides_background.htm)>.
- [23] Unites States Senate, *Subcommittee on Oceans and International Environment of the Committee on Foreign Relations, Weather Modification*, Washington, D.C., 1974.
- [24] Australian Bureau of Meteorology (2010e), *Global climate variability & change - Time series graphs – Annual Mean Surface Temperature Anomaly*, viewed 6 August 2010, <<http://www.bom.gov.au/cgi-bin/climate/change/global/timeseries.cgi>>.
- [25] Wigley, M.L., Ramaswamy, V., Christy, J.R., Lanzante, J.R., Mears, C.A., Santer, B.D., and Folland, C.K. (2006), *Temperature Trends in the Lower Atmosphere*, U.S. Global Change Research Program, Washington D.C..
- [26] Australian Bureau of Meteorology (2005), *Some Observed changes in Tasmanian rainfall and temperatures*, Tasmania and Antarctica Regional Office, Tasmania, Australia.
- [27] Mock, D. R. (1981), *The Southern Oscillation : Historical Origins*, NOAA - Skaggs, Seattle, 1968.
- [28] University of Washington JISAO (2010), *Pacific Decadal Oscillation (PDO)*, viewed 2 December 2010, <<http://jisao.washington.edu/pdo/PDO.latest>>.
- [29] NOAA Earth System Research Laboratory, *Trends in Atmospheric Carbon Dioxide*, viewed 2 August 2010, <<http://www.esrl.noaa.gov/gmd/ccgg/trends/>>.
- [30] Kuehn, K.A., Steiner, D., and Gessner, M.O. (2004), *Diel Mineralization Patterns of Standing-Dead Plant Litter: Implications for CO2 Flux from Wetlands*, Ecology, Ecological Society of America, 85(9), 2508.
- [31] Australian Bureau of Meteorology (2010f), *Climate Data Online – Monthly rainfall*, viewed 6 August 2010d, <[http://www.bom.gov.au/jsp/ncc/cdio/weatherData/av?p\\_nccObsCode=139&p\\_display\\_type=dataFile&p\\_startYear=&p\\_stn\\_num=022022](http://www.bom.gov.au/jsp/ncc/cdio/weatherData/av?p_nccObsCode=139&p_display_type=dataFile&p_startYear=&p_stn_num=022022)>.
- [32] Australian Bureau of Meteorology (2010g), *Climate Data Online – Monthly rainfall*, viewed 6 August 2010e, <[http://www.bom.gov.au/jsp/ncc/cdio/weatherData/av?p\\_nccObsCode=139&p\\_display\\_type=dataFile&p\\_startYear=&p\\_stn\\_num=021044](http://www.bom.gov.au/jsp/ncc/cdio/weatherData/av?p_nccObsCode=139&p_display_type=dataFile&p_startYear=&p_stn_num=021044)>.
- [33] Australian Bureau of Meteorology (2010h), *Climate Data Online – Monthly rainfall*, viewed 6 August 2010f, <[http://www.bom.gov.au/jsp/ncc/cdio/weatherData/av?p\\_nccObsCode=139&p\\_display\\_type=dataFile&p\\_startYear=&p\\_stn\\_num=022021](http://www.bom.gov.au/jsp/ncc/cdio/weatherData/av?p_nccObsCode=139&p_display_type=dataFile&p_startYear=&p_stn_num=022021)>.
- [34] Australian Bureau of Meteorology (2010i), *Climate Data Online – Monthly rainfall*, viewed 6 August 2010, <[http://www.bom.gov.au/jsp/ncc/cdio/weatherData/av?p\\_nccObsCode=139&p\\_display\\_type=dataFile&p\\_startYear=&p\\_stn\\_num=021129](http://www.bom.gov.au/jsp/ncc/cdio/weatherData/av?p_nccObsCode=139&p_display_type=dataFile&p_startYear=&p_stn_num=021129)>.
- [35] Australian Bureau of Meteorology (2010j), *Southern Oscillation Index*, viewed 12 January 2011, <<http://reg.bom.gov.au/climate/current/soi2.shtml>>.